Cosmology from the Abundance of Massive Halos: SPT Clusters with DES and HST Weak Lensing

Sebastian Bocquet, LMU Munich

with Sebastian Grandis, Lindsey Bleem, Matthias Klein, Joe Mohr, Tim Schrabback
and the *South Pole Telescope* (SPT) and *Dark Energy Survey* (DES) collaborations

Image credit: SPT 2024 winter-overs Josh + Kevin

Massive Halos ≳ 10^{14} *M*sun

… trace the large-scale structure

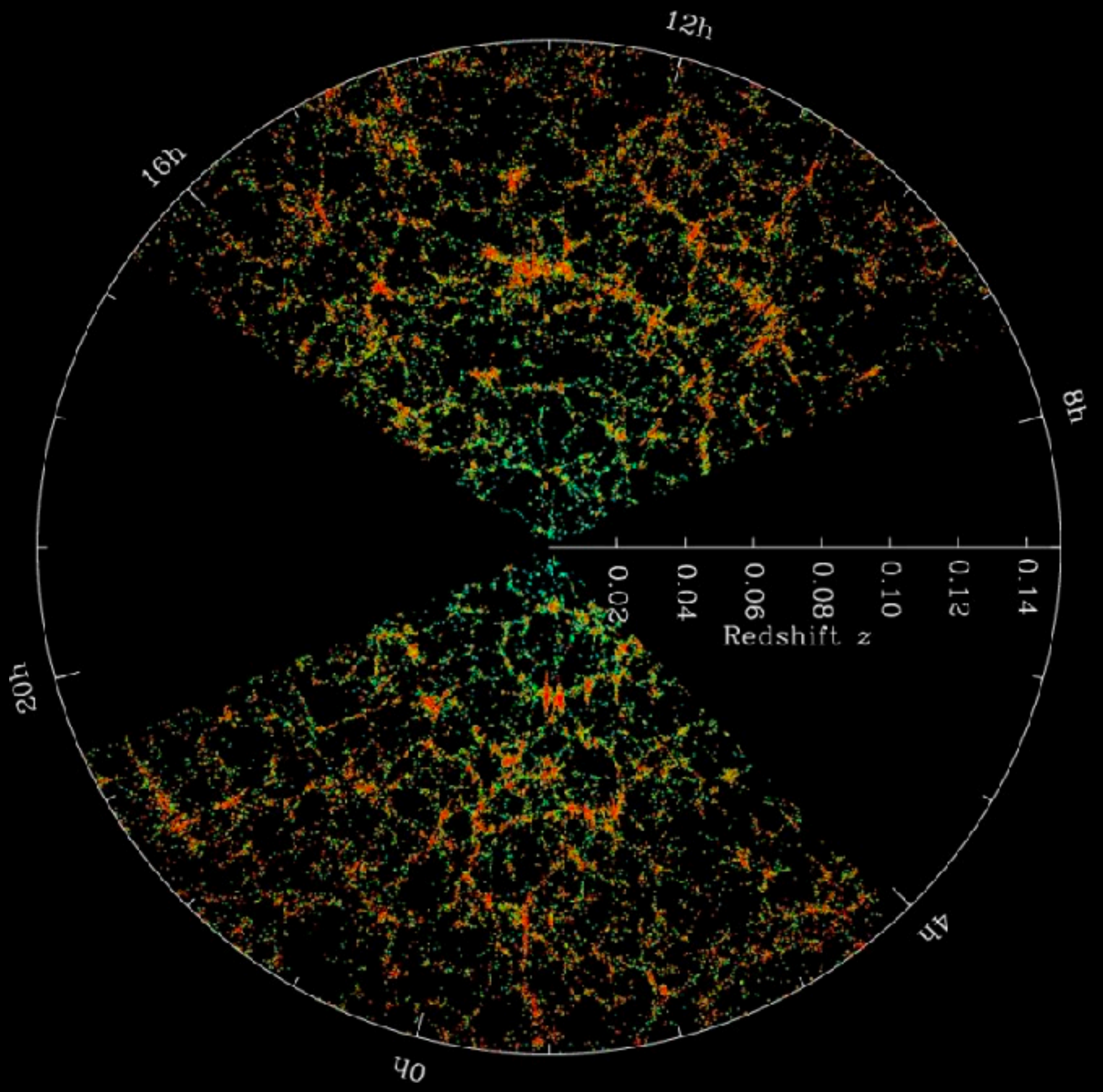

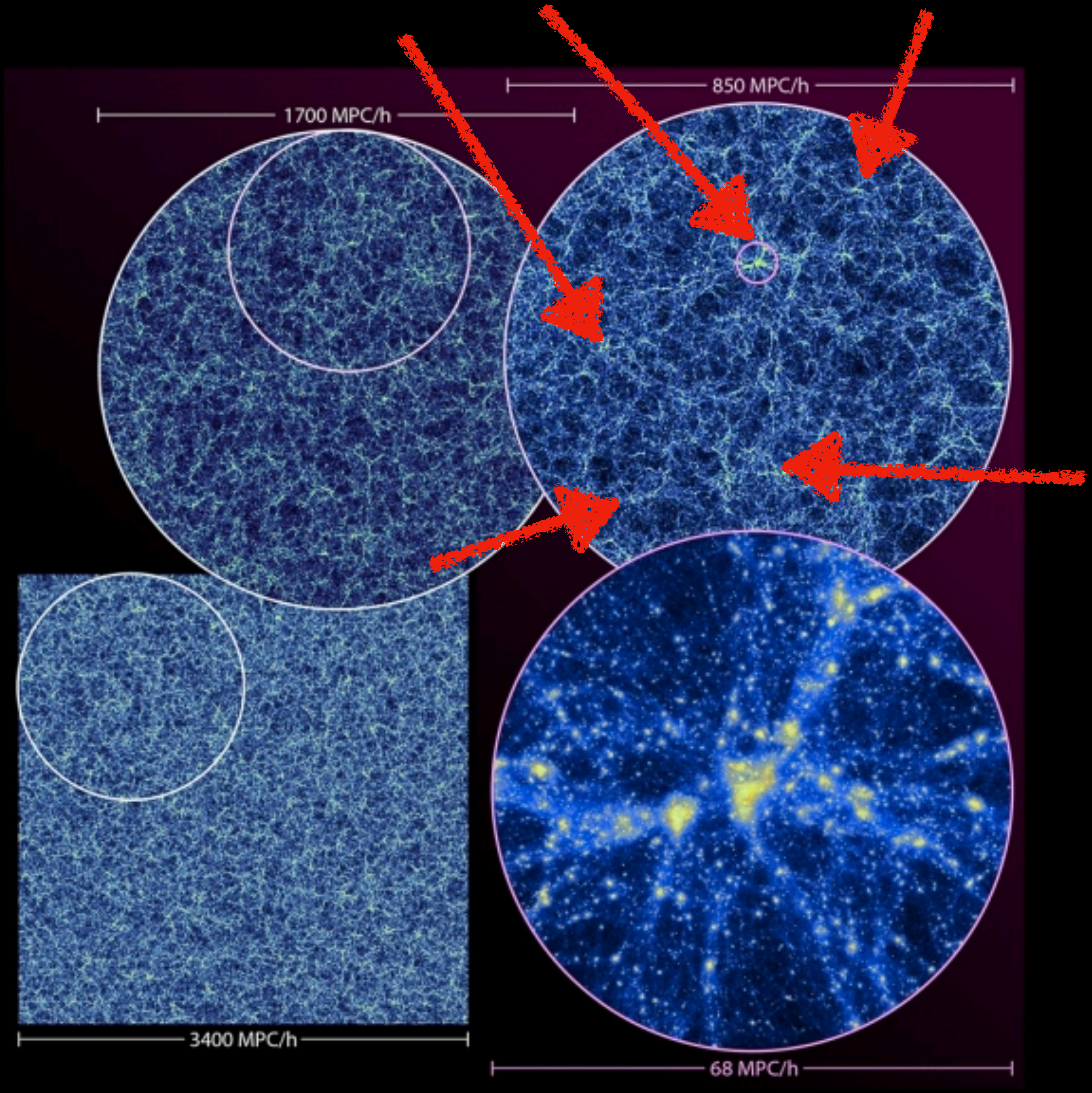

Last Journey (on Mira supercomputer) (Heitmann+)

Cluster Cosmology

The most massive collapsed objects $\gtrsim 10^{14}\ M_\odot$

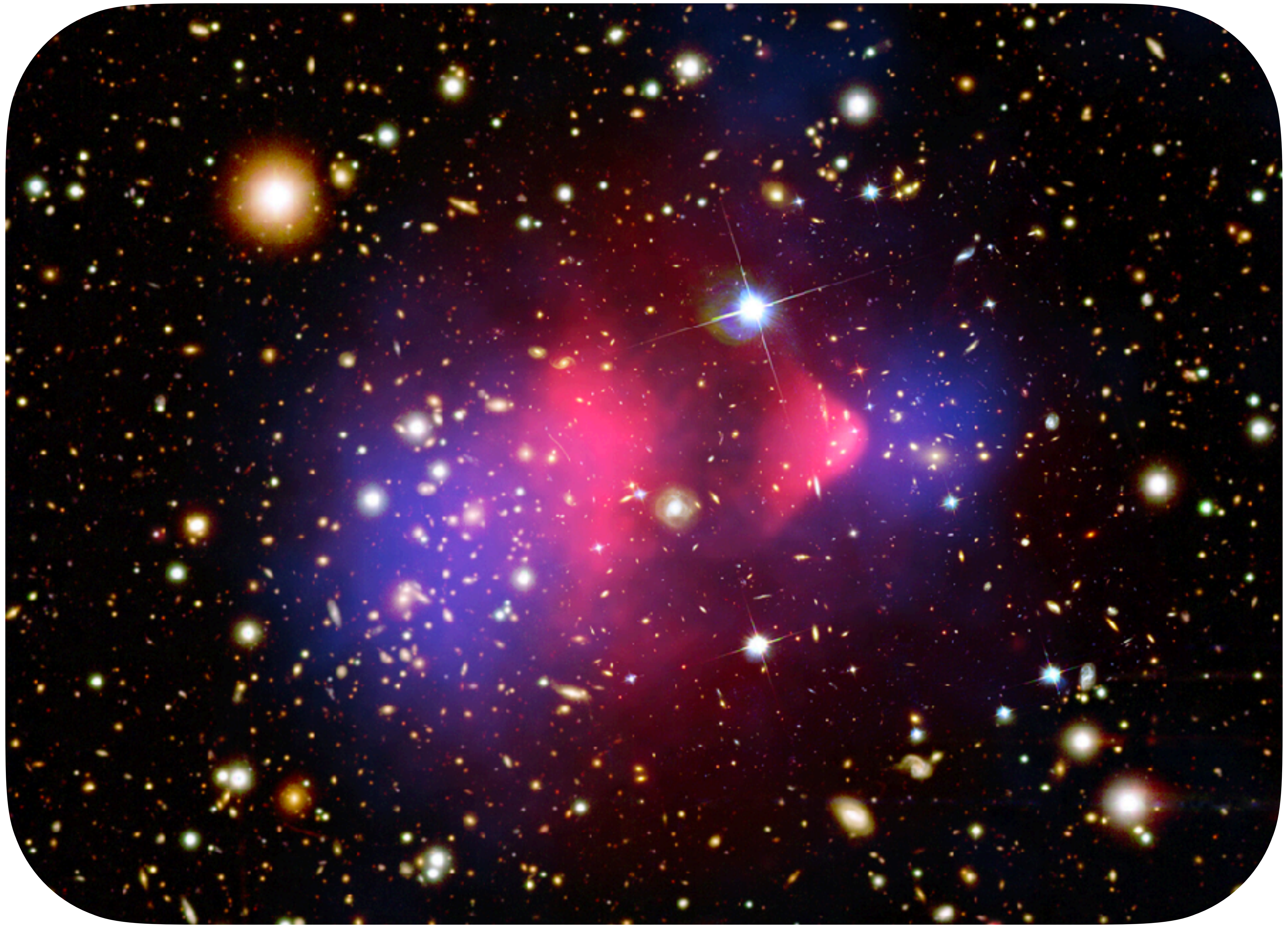

Bullet Cluster. X-ray: NASA/CXC/CfA/M.Markevitch, Optical and lensing map: NASA/STScI, Magellan/U.Arizona/D.Clowe, Lensing map: ESO WFI

- Composition
  - 85—90% dark matter
  - 10—15% ordinary matter, of which
    - ~ 75% (gravitationally heated) gas
    - ~ 25% galaxies/stars
- Somewhat arbitrary (but useful) definition
  - Halo ≡ *entire* thing
  - Cluster ≡ galaxies & gas (what we see)

Large-Scale Structure and Cosmology

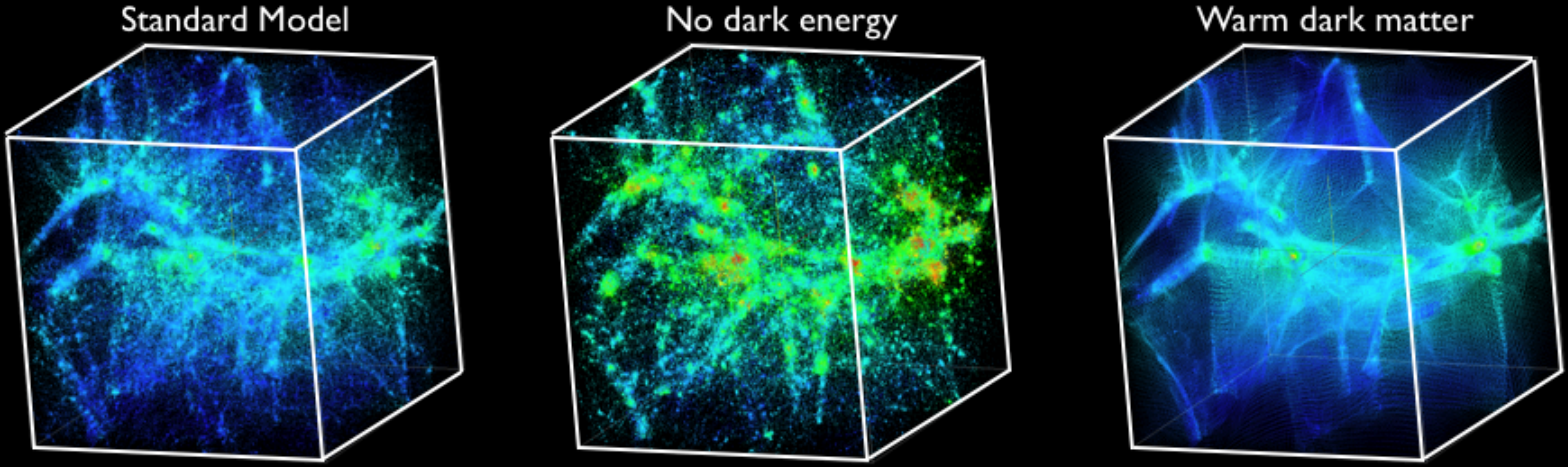

Credit: Katrin Heitmann

Halo Mass Function

d*N(z)*/dln*M* — vanilla ΛCDM cosmology

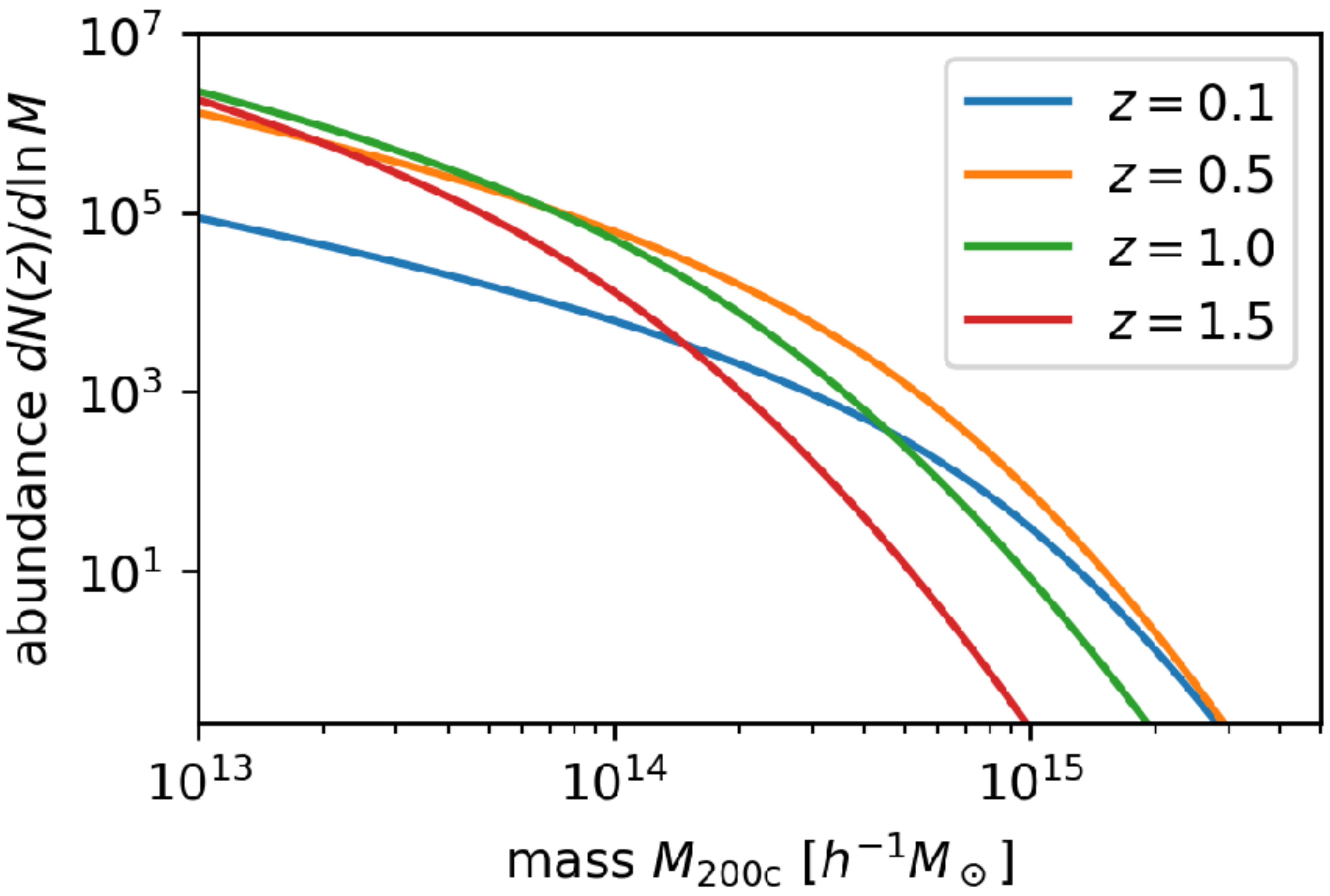

Halo Mass Function

d*N(z)*/dln*M* — now *w* = -1.1 (instead of -1)

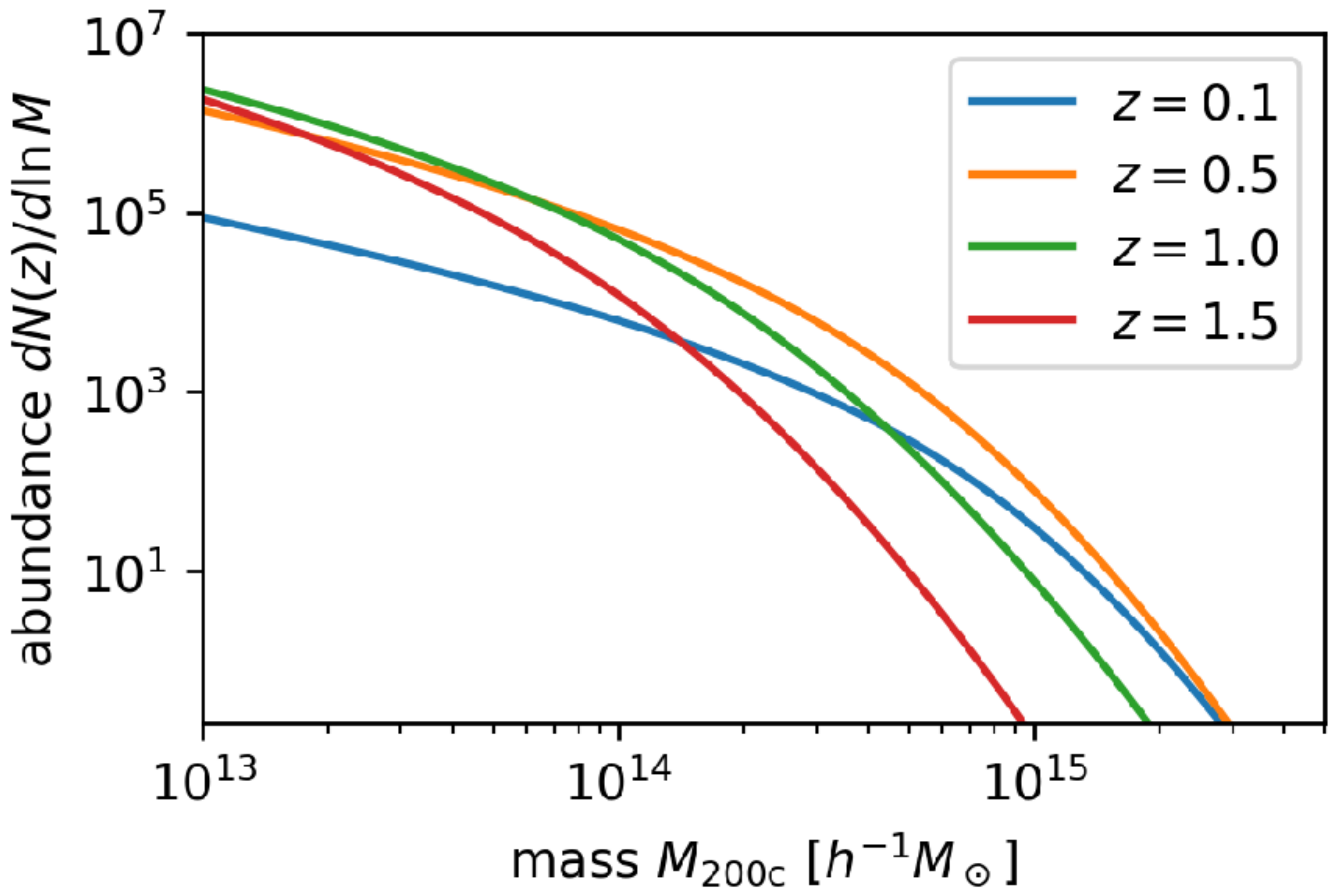

Halo Mass Function

Impact of changing dark energy equation of state parameter by 0.1

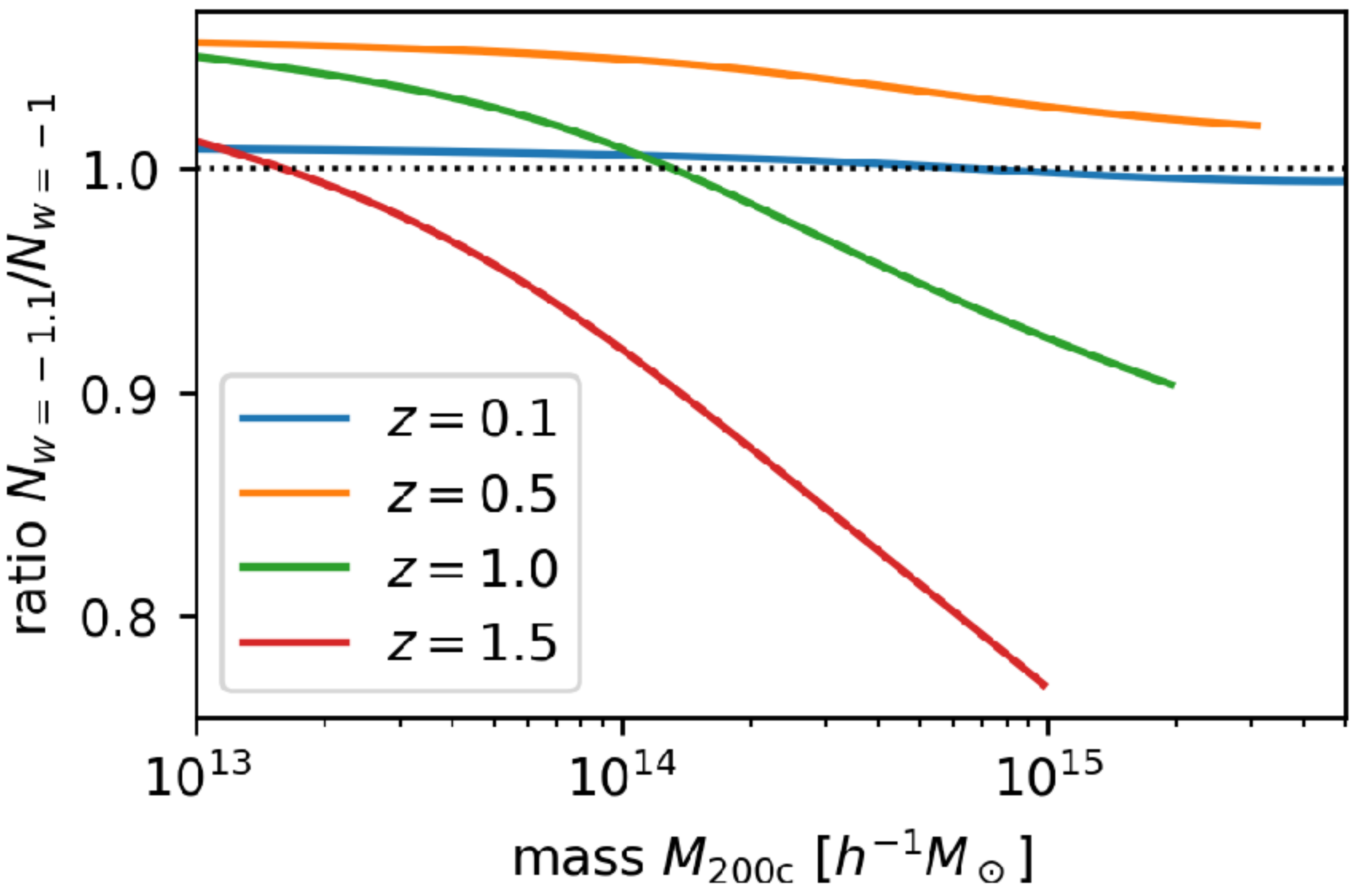

Back to reality

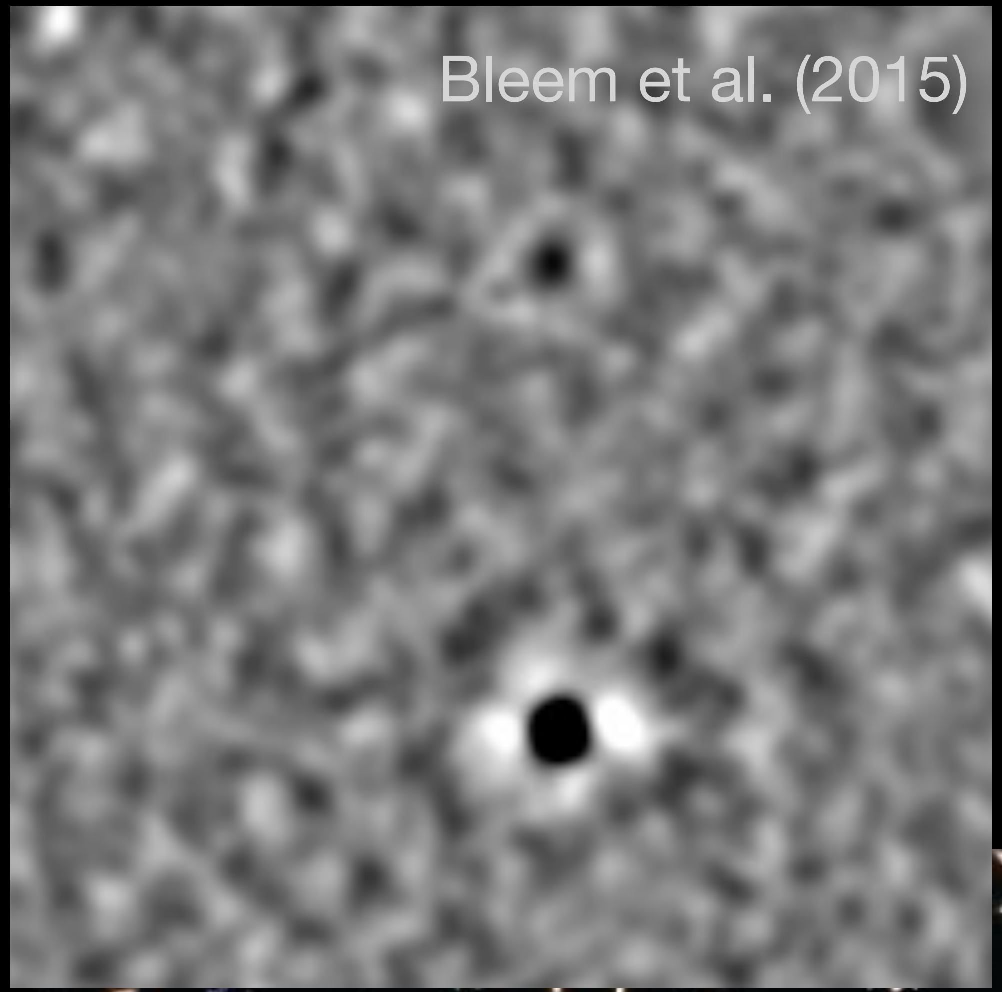

Credit: NASA, ESA, and J. Lotz, M. Mountain, A. Koekemoer, and the HFF Team (STScI) http://www.spacetelescope.org/images/heic1401a/

Credit: NASA, ESA, the Hubble Heritage Team (STScI/AURA), J. Blakeslee (NRC Herzberg Astrophysics Program, Dominion Astrophysical Observatory), and H. Ford (JHU) http://www.spacetelescope.org/images/heic1317a

“Halo Observable Function”

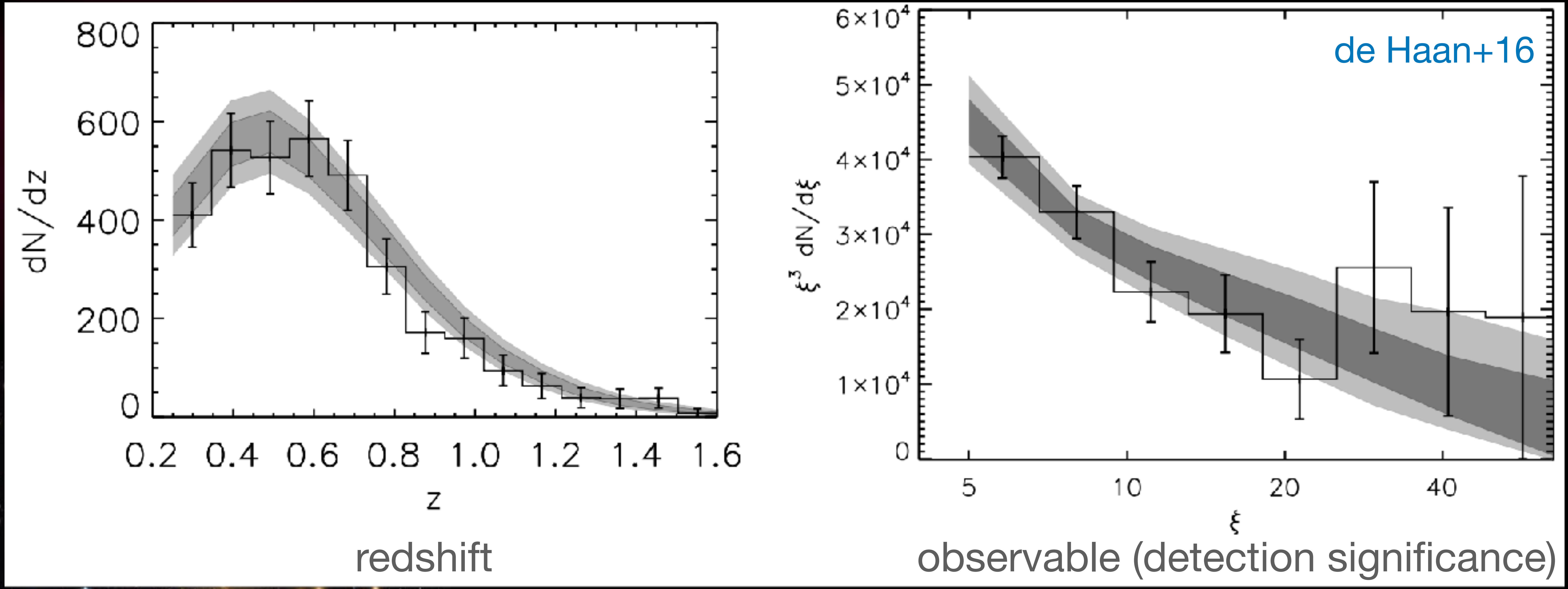

Observable vs. Mass

halo observable function

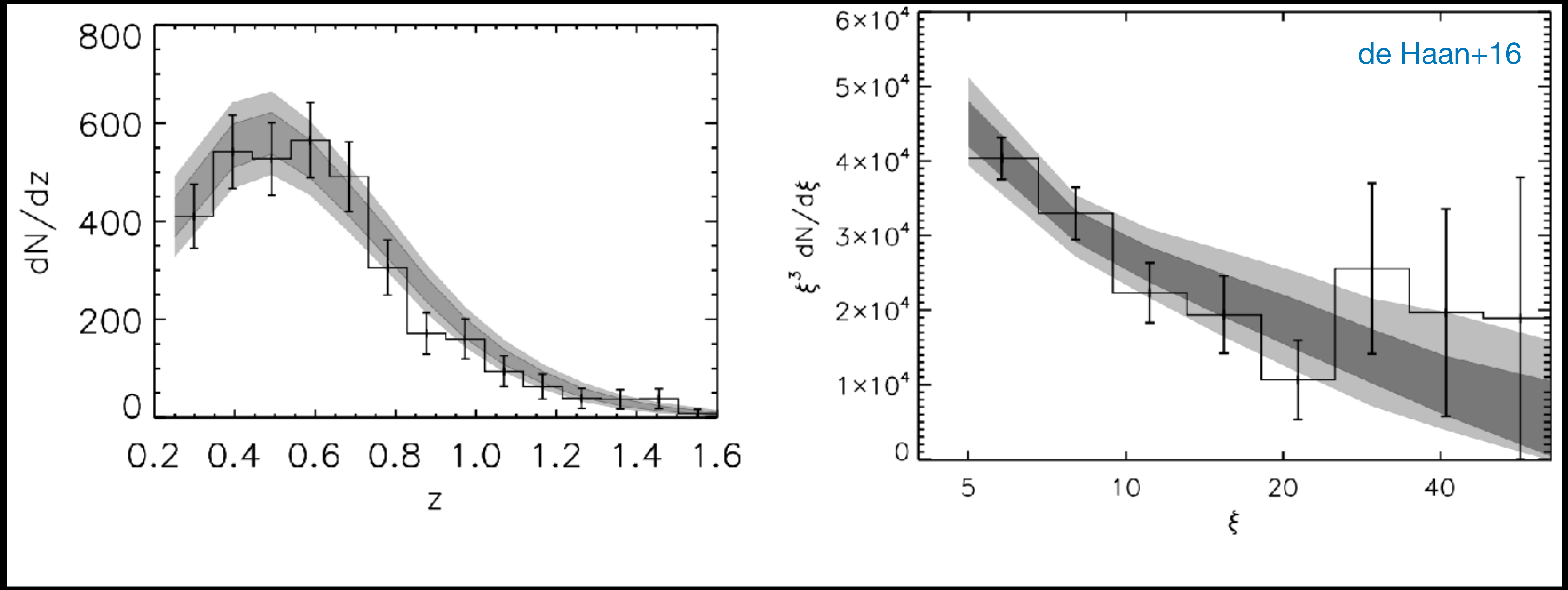

clusters

halos

halo mass function

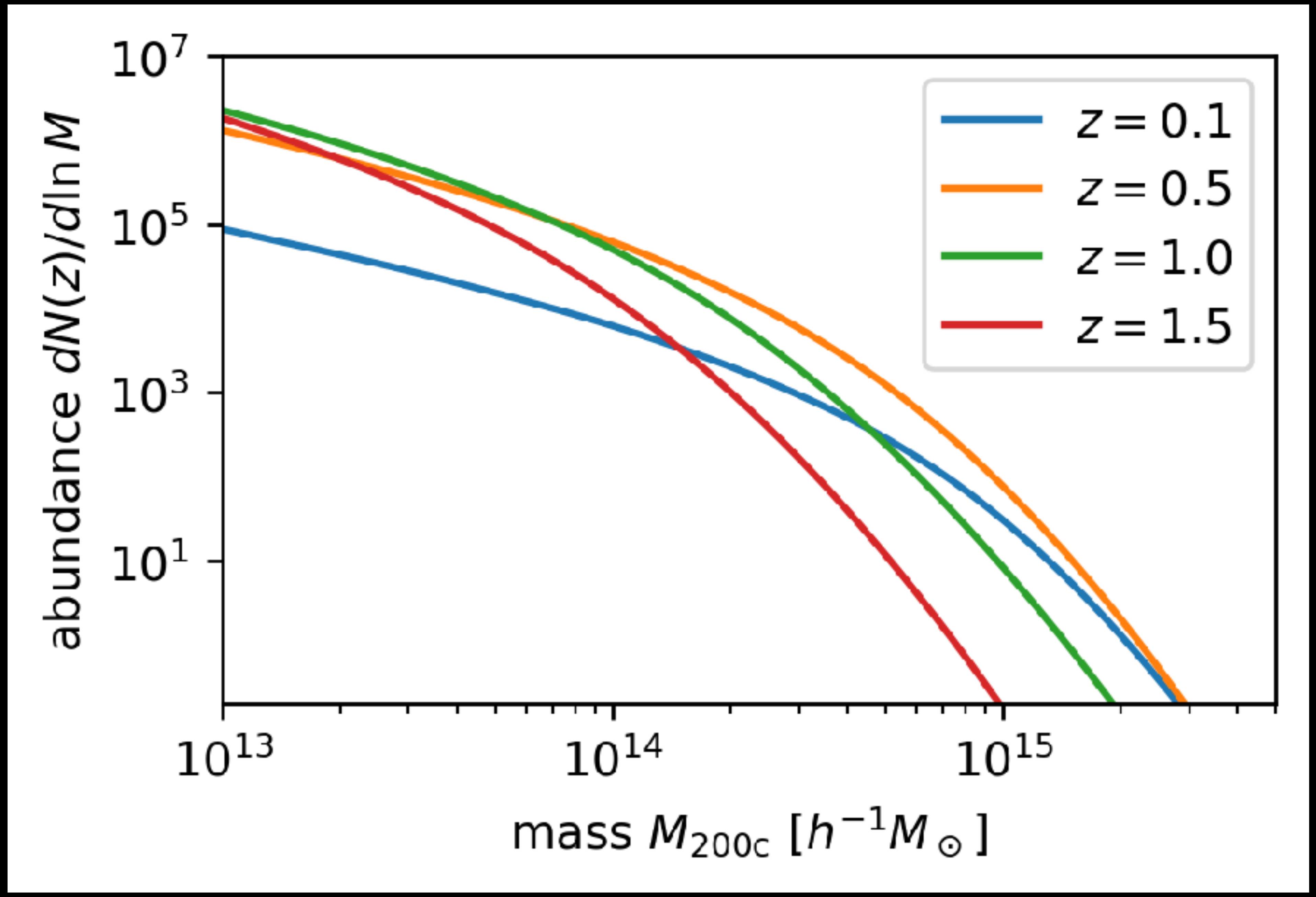

observable—mass relation

$$\frac{dN}{d\mathrm{obs}} = \int dM \, P(\mathrm{obs}\,|\,M) \, \frac{dN}{dM}$$

halo mass function

cluster cosmology = cluster selection + mass calibration

Modeling Framework

Observable—Mass Relations

- The bigger a halo, the stronger its SZ, X-ray, optical, lensing signal
  - Supported by theory and numerical simulations
  - These are average relations — there is intrinsic scatter, because no two objects are the same
- For the experts:
  - Halo morphology and evolution lead to correlated scatter among observables

Simulations (Angulo+12)

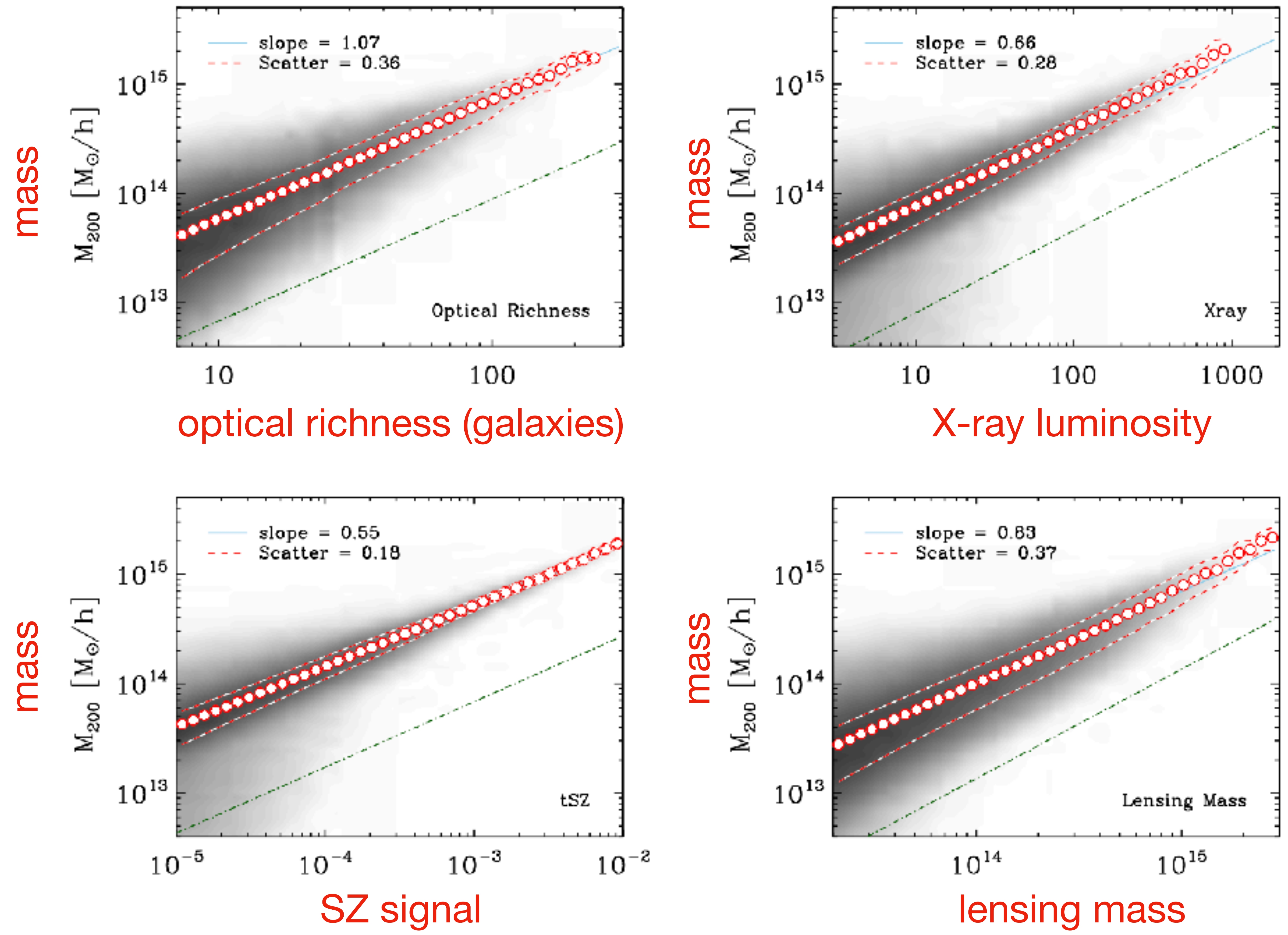

Mass Calibration I

How do the observables relate to halo mass?

- We *could* use predictions from first principles (e.g., hydrostatic equilibrium) or numerical simulations
    - Systematically limited by uncertain astrophysics
- Weak-lensing-to-mass relation is known within few percents

Idealized (exaggerated) situation

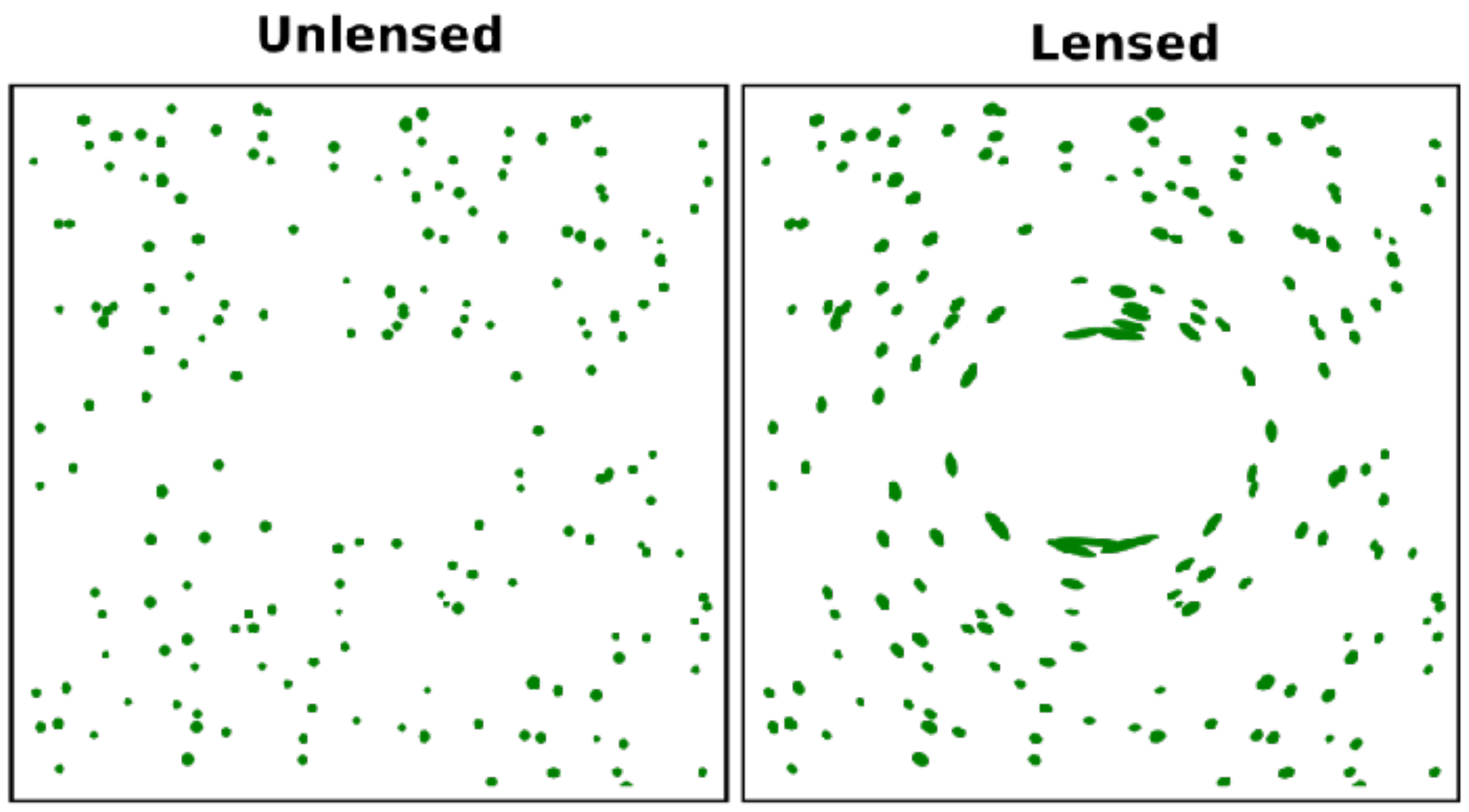

By TallJimbo - Own work, CC BY-SA 3.0, https://commons.wikimedia.org/w/index.php?curid=4150002

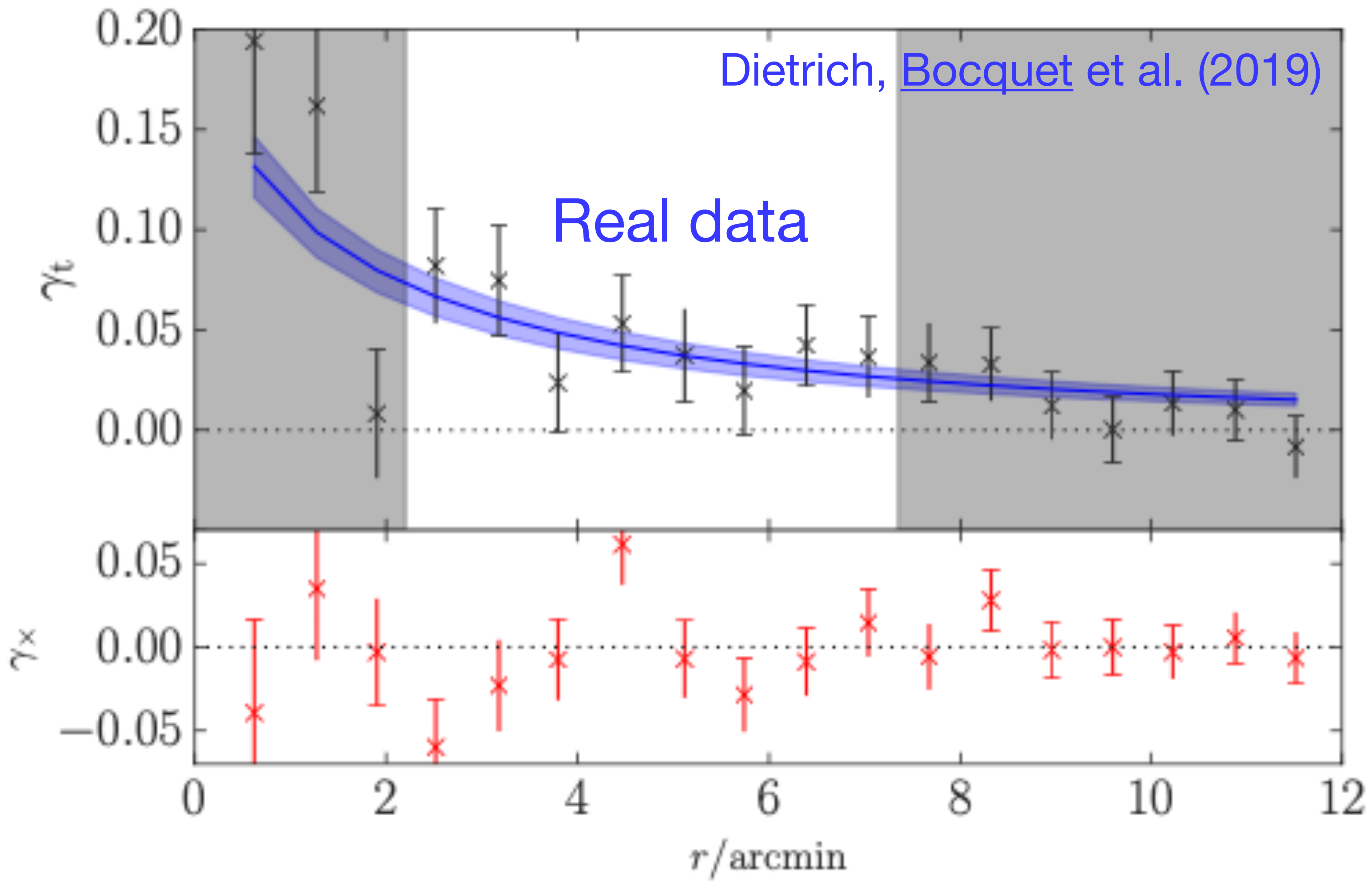

(b) Tangential shear profile of SPT-CL J0254−5857.

Mass Calibration II. Weak Lensing

Robust observable—mass relations

- We *could* use predictions from first principles (e.g., hydrostatic equilibrium) or numerical simulations
    - Systematically limited by uncertain astrophysics
- Weak-lensing-to-mass relation is known within few percents
    - Used to demonstrate that **hydrostatic mass ≠ halo mass**
    - **With lensing** measurements of sample clusters, ***we empirically* calibrate the observable—mass relations**

Medezinski+ 18

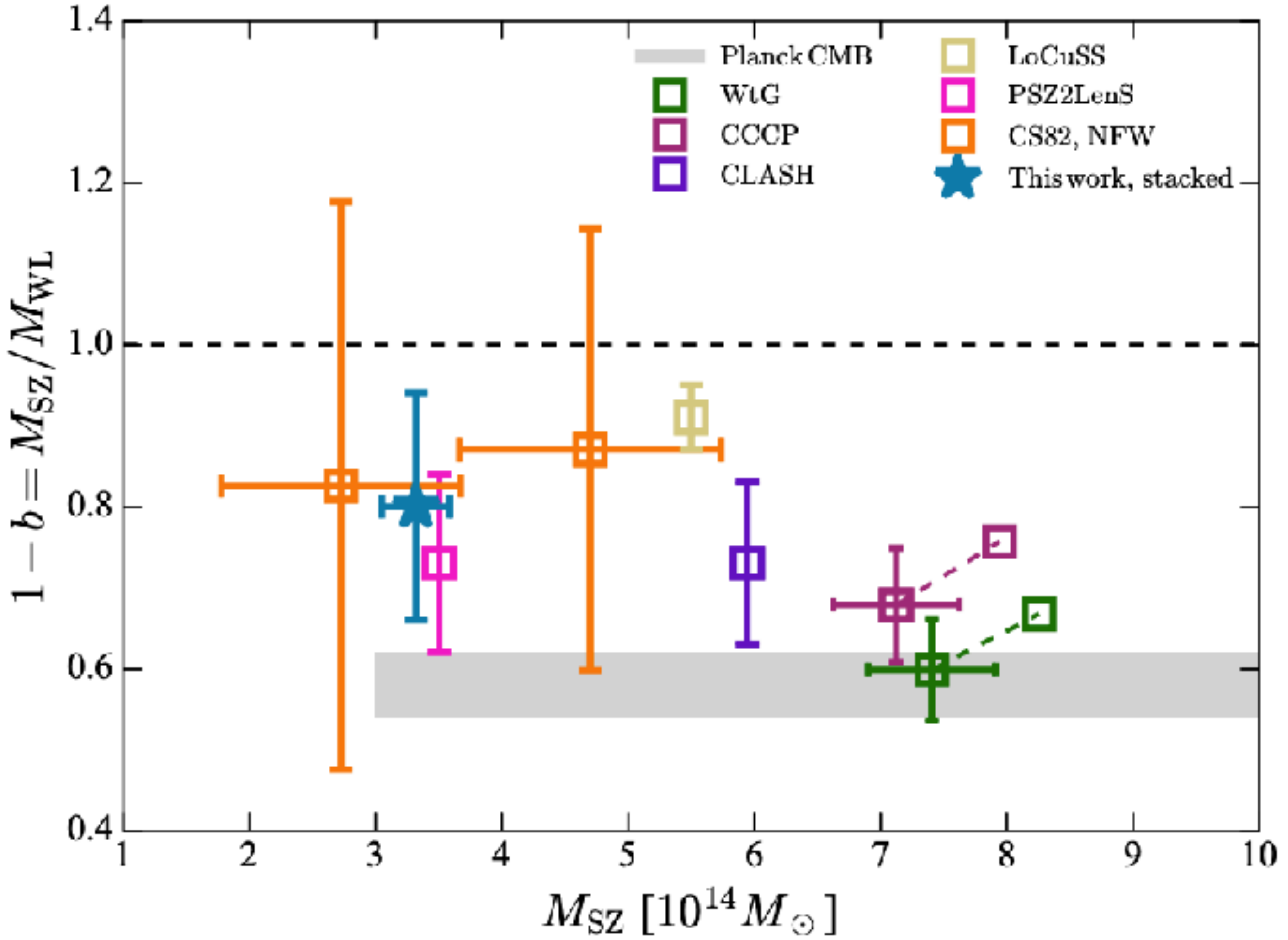

SPT Clusters with DES and HST Weak Lensing. I. Cluster Lensing and Bayesian Population Modeling of Multi-Wavelength Cluster Datasets

S. Bocquet,[1,*] S. Grandis,[2,1] L. E. Bleem,[3,4] M. Klein,[1] J. J. Mohr,[1,5] M. Aguena,[6] A. Alarcon,[3] S. Allam,[7] S. W. Allen,[8,9,10] O. Alves,[11] A. Amon,[12,13] B. Ansarinejad,[14] D. Bacon,[15] M. Bayliss,[16] K. Bechtol,[17] M. R. Becker,[3] B. A. Benson,[18,4,19] G. M. Bernstein,[20] M. Brodwin,[21] D. Brooks,[22] A. Campos,[23] R. E. A. Canning,[24] J. E. Carlstrom,[18,4,25,3,26] A. Carnero Rosell,[27,6,28] M. Carrasco Kind,[29,30] J. Carretero,[31] R. Cawthon,[32] C. Chang,[18,4] R. Chen,[33] A. Choi,[34] J. Cordero,[35] M. Costanzi,[36,37,38] L. N. da Costa,[6] M. E. S. Pereira,[39] C. Davis,[40] J. DeRose,[41] S. Desai,[42] T. de Haan,[43,44] J. De Vicente,[45] H. T. Diehl,[7] S. Dodelson,[23,46] P. Doel,[22] C. Doux,[20,47] A. Drlica-Wagner,[18,7,4] K. Eckert,[20] J. Elvin-Poole,[48] S. Everett,[49] I. Ferrero,[50] A. Ferté,[51] A. M. Flores,[9,8] J. Frieman,[7,4] J. García-Bellido,[52] M. Gatti,[20] G. Giannini,[31] M. D. Gladders,[18,4] D. Gruen,[1] R. A. Gruendl,[29,30] I. Harrison,[53] W. G. Hartley,[54] K. Herner,[7] S. R. Hinton,[55] D. L. Hollowood,[56] W. L. Holzapfel,[57] K. Honscheid,[58,59] N. Huang,[57] E. M. Huff,[49] D. J. James,[60] M. Jarvis,[20] G. Khullar,[4,18] K. Kim,[16] R. Kraft,[61] K. Kuehn,[62,63] N. Kuropatkin,[7] F. Kéruzoré,[3] S. Lee,[49] P.-F. Leget,[40] N. MacCrann,[64] G. Mahler,[65,66] A. Mantz,[8,9] J. L. Marshall,[67] J. McCullough,[40] M. McDonald,[68] J. Mena-Fernández,[45] R. Miquel,[69,31] J. Myles,[9,40,51] A. Navarro-Alsina,[70] R. L. C. Ogando,[71] A. Palmese,[23] S. Pandey,[20] A. Pieres,[6,71] A. A. Plazas Malagón,[40,51] J. Prat,[18,4] M. Raveri,[72] C. L. Reichardt,[14] J. Roberson,[16] R. P. Rollins,[35] A. K. Romer,[73] C. Romero,[74] A. Roodman,[40,51] A. J. Ross,[58] E. S. Rykoff,[40,51] L. Salvati,[75,76,77] C. Sánchez,[20] E. Sanchez,[45] D. Sanchez Cid,[45] A. Saro,[78,77,76,79,80] T. Schrabback,[81,2] M. Schubnell,[11] L. F. Secco,[4] I. Sevilla-Noarbe,[45] K. Sharon,[82] E. Sheldon,[83] T. Shin,[84] M. Smith,[85] T. Somboonpanyakul,[86,40] B. Stalder,[61] A. A. Stark,[61] V. Strazzullo,[76,87,77] E. Suchyta,[88] M. E. C. Swanson,[29] G. Tarle,[11] C. To,[58] M. A. Troxel,[33] I. Tutusaus,[89] T. N. Varga,[90,5,91] A. von der Linden,[84] N. Weaverdyck,[11,41] J. Weller,[5,91] P. Wiseman,[85] B. Yanny,[7] B. Yin,[23] M. Young,[92] Y. Zhang,[93] and J. Zuntz[94]
(the DES and SPT Collaborations)

arXiv:2310:12213 — PRD accepted

SPT Clusters with DES and HST Weak Lensing. II. Cosmological Constraints from the Abundance of Massive Halos

S. Bocquet,[1,*] S. Grandis,[2,1] L. E. Bleem,[3,4] M. Klein,[1] J. J. Mohr,[1,5] T. Schrabback,[2,6] T. M. C. Abbott,[7] P. A. R. Ade,[8] M. Aguena,[9] A. Alarcon,[3] S. Allam,[10] S. W. Allen,[11,12,13] O. Alves,[14] A. Amon,[15,16] A. J. Anderson,[10] J. Annis,[10] B. Ansarinejad,[17] J. E. Austermann,[18,19] S. Avila,[20] D. Bacon,[21] M. Bayliss,[22] J. A. Beall,[18] K. Bechtol,[23] M. R. Becker,[3] A. N. Bender,[3,4,24] B. A. Benson,[24,4,10] G. M. Bernstein,[25] S. Bhargava,[26] F. Bianchini,[11,12,13] M. Brodwin,[27] D. Brooks,[28] L. Bryant,[29] A. Campos,[30] R. E. A. Canning,[31] J. E. Carlstrom,[24,4,32,3,29] A. Carnero Rosell,[33,9,34] M. Carrasco Kind,[35,36] J. Carretero,[20] F. J. Castander,[37,38] R. Cawthon,[39] C. L. Chang,[4,3,24] C. Chang,[24,4] P. Chaubal,[17] R. Chen,[40] H. C. Chiang,[41,42] A. Choi,[43] T-L. Chou,[4,32] R. Citron,[44] C. Corbett Moran,[45] J. Cordero,[46] M. Costanzi,[47,48,49] T. M. Crawford,[4,24] A. T. Crites,[50] L. N. da Costa,[9] M. E. S. Pereira,[51] C. Davis,[11] T. M. Davis,[52] J. DeRose,[53] S. Desai,[54] T. de Haan,[55,56] H. T. Diehl,[10] M. A. Dobbs,[41,57] S. Dodelson,[30,58] C. Doux,[25,59] A. Drlica-Wagner,[24,10,4] K. Eckert,[25] J. Elvin-Poole,[60] S. Everett,[61] W. Everett,[62] I. Ferrero,[63] A. Ferté,[13] A. M. Flores,[12,11] J. Frieman,[10,4] J. Gallicchio,[4,64] J. García-Bellido,[65] M. Gatti,[25] E. M. George,[66] G. Giannini,[20,4] M. D. Gladders,[24,4] D. Gruen,[1] R. A. Gruendl,[35,36] N. Gupta,[67] G. Gutierrez,[10] N. W. Halverson,[62,19] I. Harrison,[68] W. G. Hartley,[69] K. Herner,[10] S. R. Hinton,[52] G. P. Holder,[36,70,57] D. L. Hollowood,[71] W. L. Holzapfel,[72] K. Honscheid,[73,74] J. D. Hrubes,[44] N. Huang,[72] J. Hubmayr,[18] E. M. Huff,[61] D. Huterer,[14] K. D. Irwin,[13,12] D. J. James,[75] M. Jarvis,[25] G. Khullar,[4,24] K. Kim,[22] L. Knox,[76] R. Kraft,[75] . Krause,[77] K. Kuehn,[78,79] N. Kuropatkin,[10] F. Kéruzoré,[3] O. Lahav,[28] A. T. Lee,[72,80] P.-F. Leget,[81] D. Li,[18,13] H. Lin,[10] A. Lowitz,[24] N. MacCrann,[82] G. Mahler,[83,84] A. Mantz,[11,12] J. L. Marshall,[85] J. McCullough,[81] M. McDonald,[86] J. J. McMahon,[4,32,24] J. Mena-Fernández,[87] F. Menanteau,[35,36] S. S. Meyer,[4,32,24,29] R. Miquel,[88,20] J. Montgomery,[41] J. Myles,[89] T. Natoli,[24,4] A. Navarro-Alsina,[90] J. P. Nibarger,[18] G. I. Noble,[91] V. Novosad,[92] R. L. C. Ogando,[93] Y. Omori,[4] S. Padin,[94] S. Pandey,[25] P. Paschos,[29] S. Patil,[17] A. Pieres,[9,93] A. A. Plazas Malagón,[81,13] A. Porredon,[95] J. Prat,[24,4] C. Pryke,[96] M. Raveri,[97] C. L. Reichardt,[17] J. Roberson,[22] R. P. Rollins,[46] C. Romero,[75] A. Roodman,[81,13] J. E. Ruhl,[98] E. S. Rykoff,[81,13] B. R. Saliwanchik,[99] L. Salvati,[100,101,102] C. Sánchez,[25] E. Sanchez,[103] D. Sanchez Cid,[103] A. Saro,[104,102,101,105,106] K. K. Schaffer,[4,29,107] L. F. Secco,[4] I. Sevilla-Noarbe,[103] K. Sharon,[108] E. Sheldon,[109] T. Shin,[110] C. Sievers,[44] G. Smecher,[41,111] M. Smith,[112] T. Somboonpanyakul,[113] M. Sommer,[6] B. Stalder,[75] A. A. Stark,[75] J. Stephen,[29] V. Strazzullo,[101,102] E. Suchyta,[114] G. Tarle,[14] C. To,[73] M. A. Troxel,[40] C. Tucker,[8] I. Tutusaus,[115] T. N. Varga,[116,5,117] T. Veach,[118] J. D. Vieira,[36,70] A. Vikhlinin,[75] A. von der Linden,[110] G. Wang,[3] N. Weaverdyck,[14,53] J. Weller,[5,117] N. Whitehorn,[119] W. L. K. Wu,[13] B. Yanny,[10] V. Yefremenko,[3] B. Yin,[30] M. Young,[91] J. A. Zebrowski,[4,24,10] Y. Zhang,[7] H. Zohren,[6] and J. Zuntz[120]
(the SPT and DES Collaborations)

arXiv:2401.02075 — PRD accepted

Image credit: SPT 2018 winter-overs Adam & Joshua

The South Pole Telescope (SPT)

10-meter sub-mm quality wavelength telescope

90, 150, 220 GHz and
1.6, 1.2, 1.0 arcmin resolution

2007: SPT-SZ
960 detectors
90,150,220 GHz

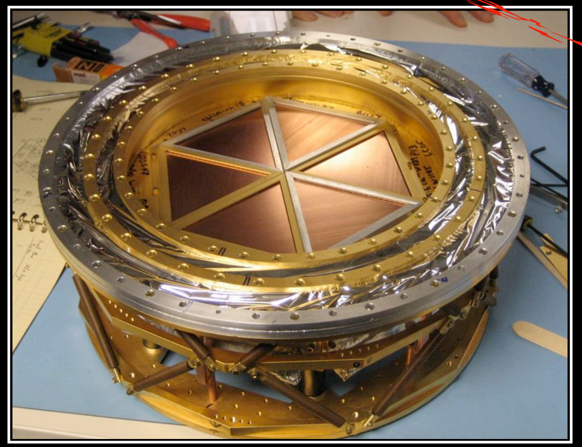

2012: SPTpol
1600 detectors
90,150 GHz
+Polarization

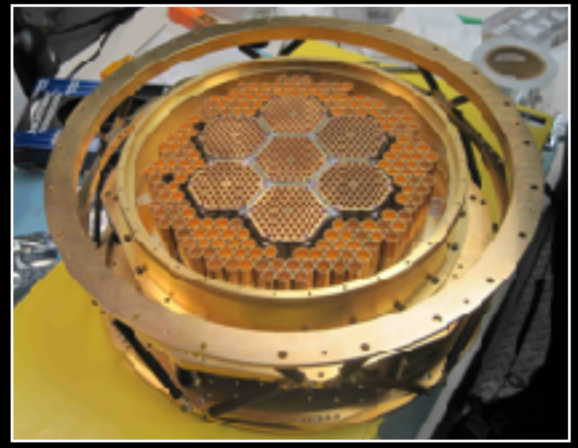

2017: SPT-3G
~15,200 detectors
90,150,220 GHz
+Polarization

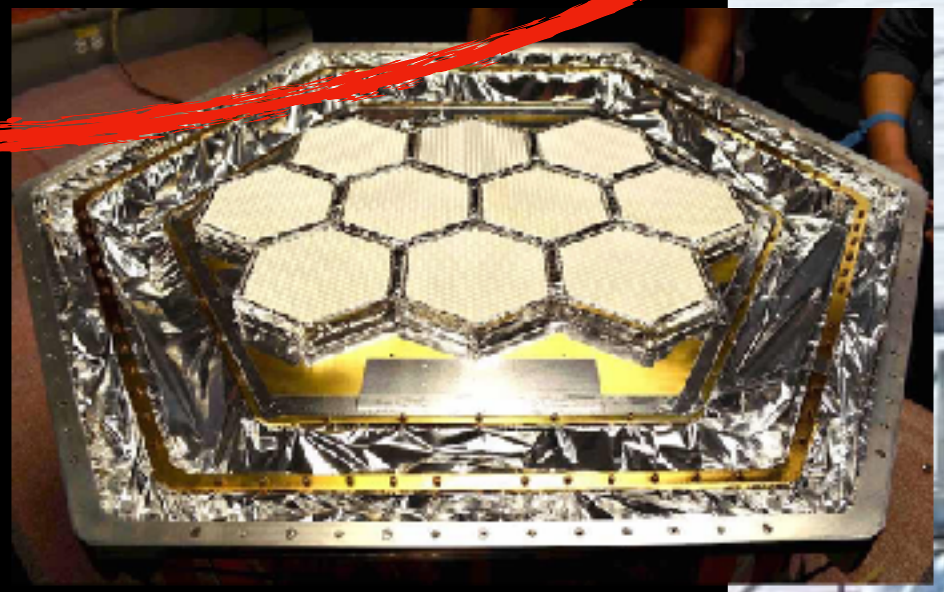

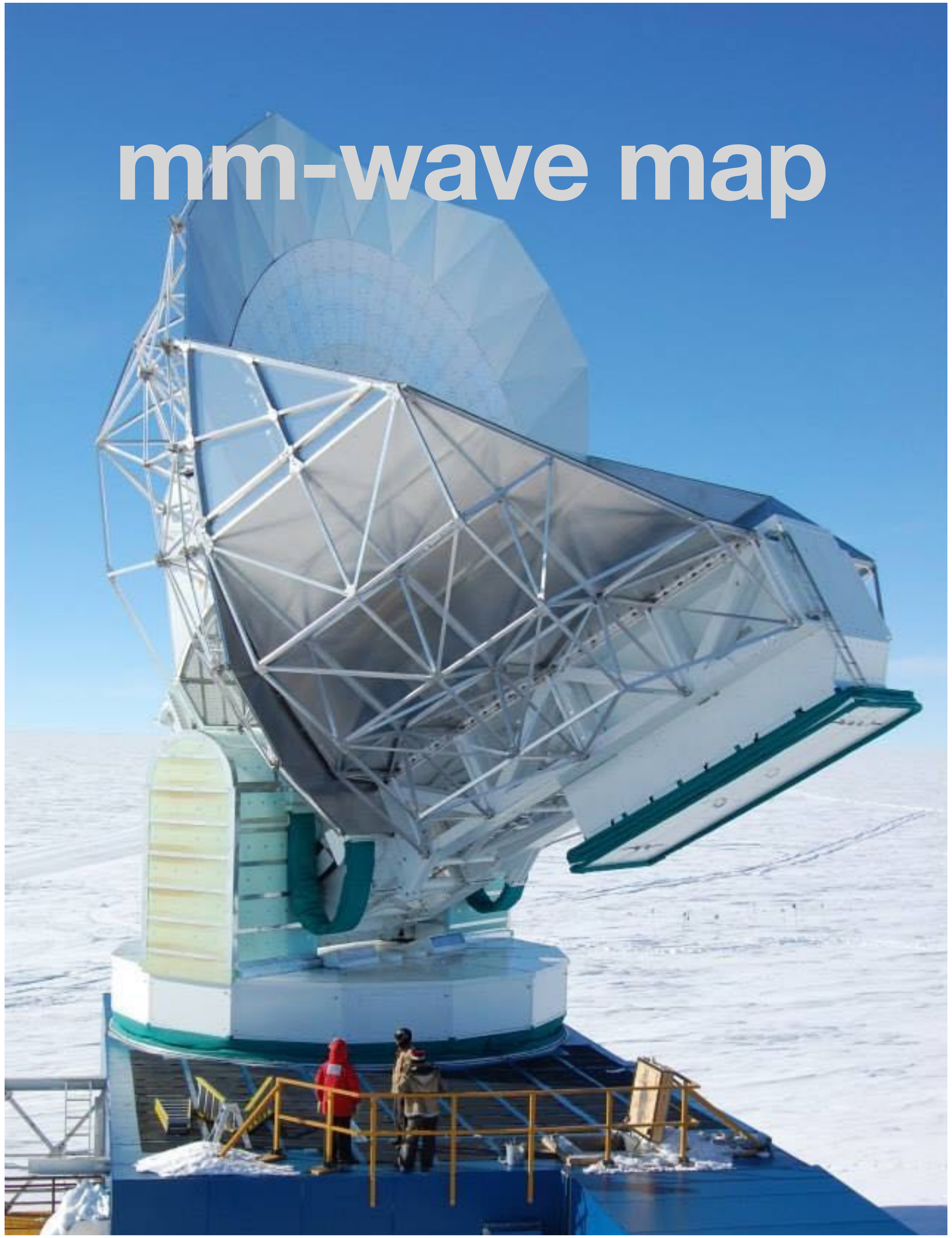
mm-wave map

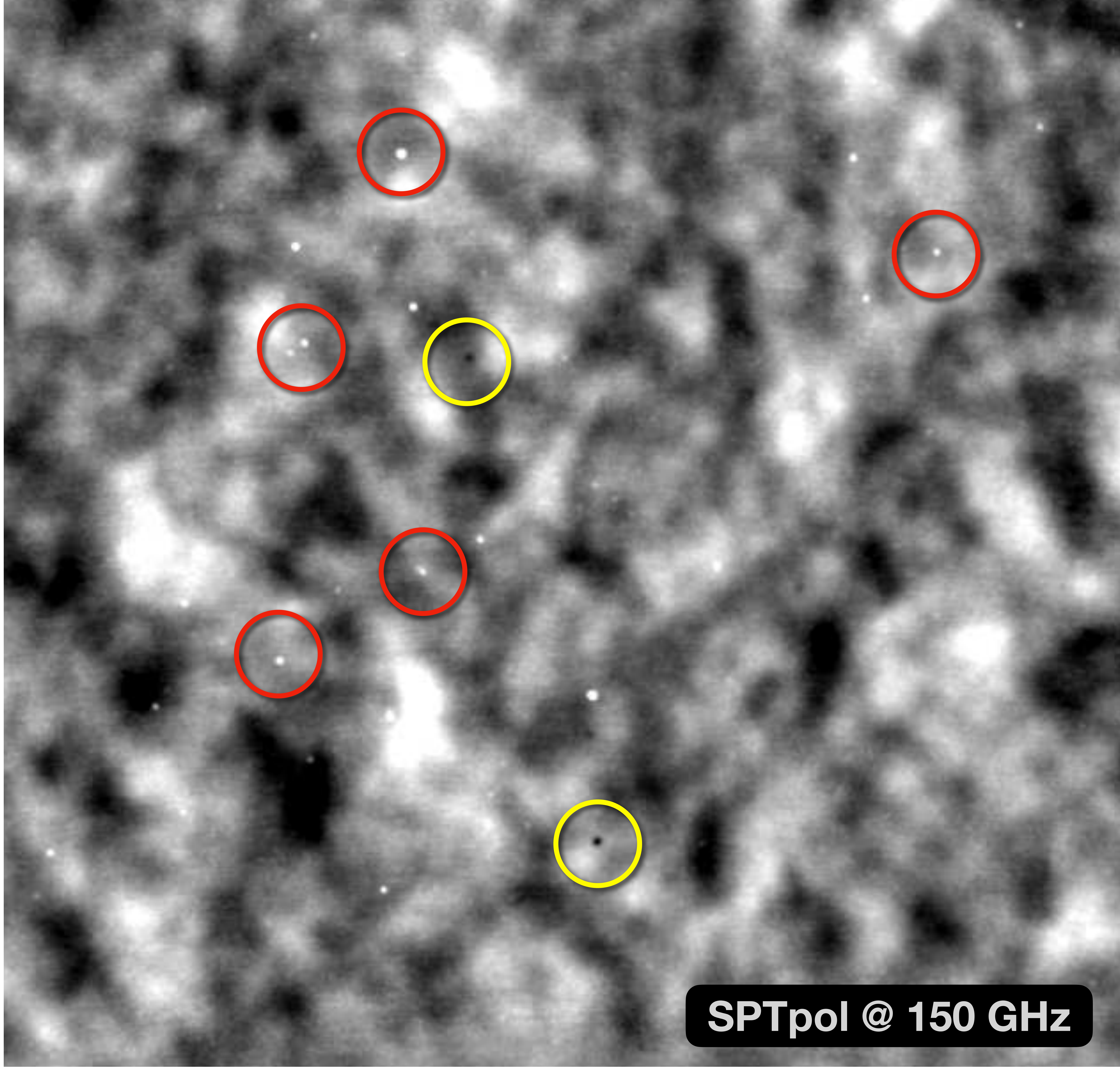
SPTpol @ 150 GHz

Find clusters

Sunyaev-Zel'dovich (SZ) Effect

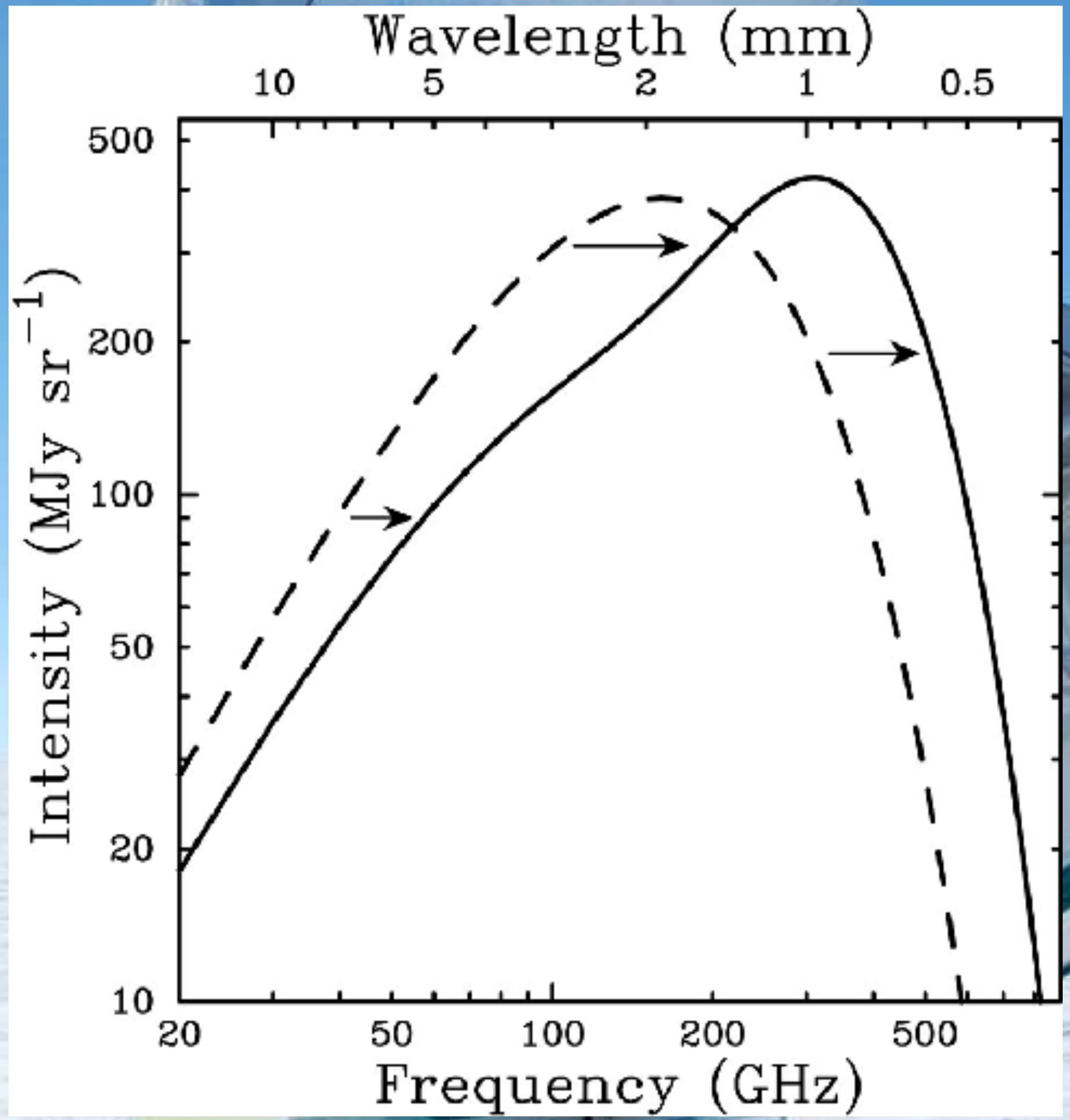

CMB spectrum

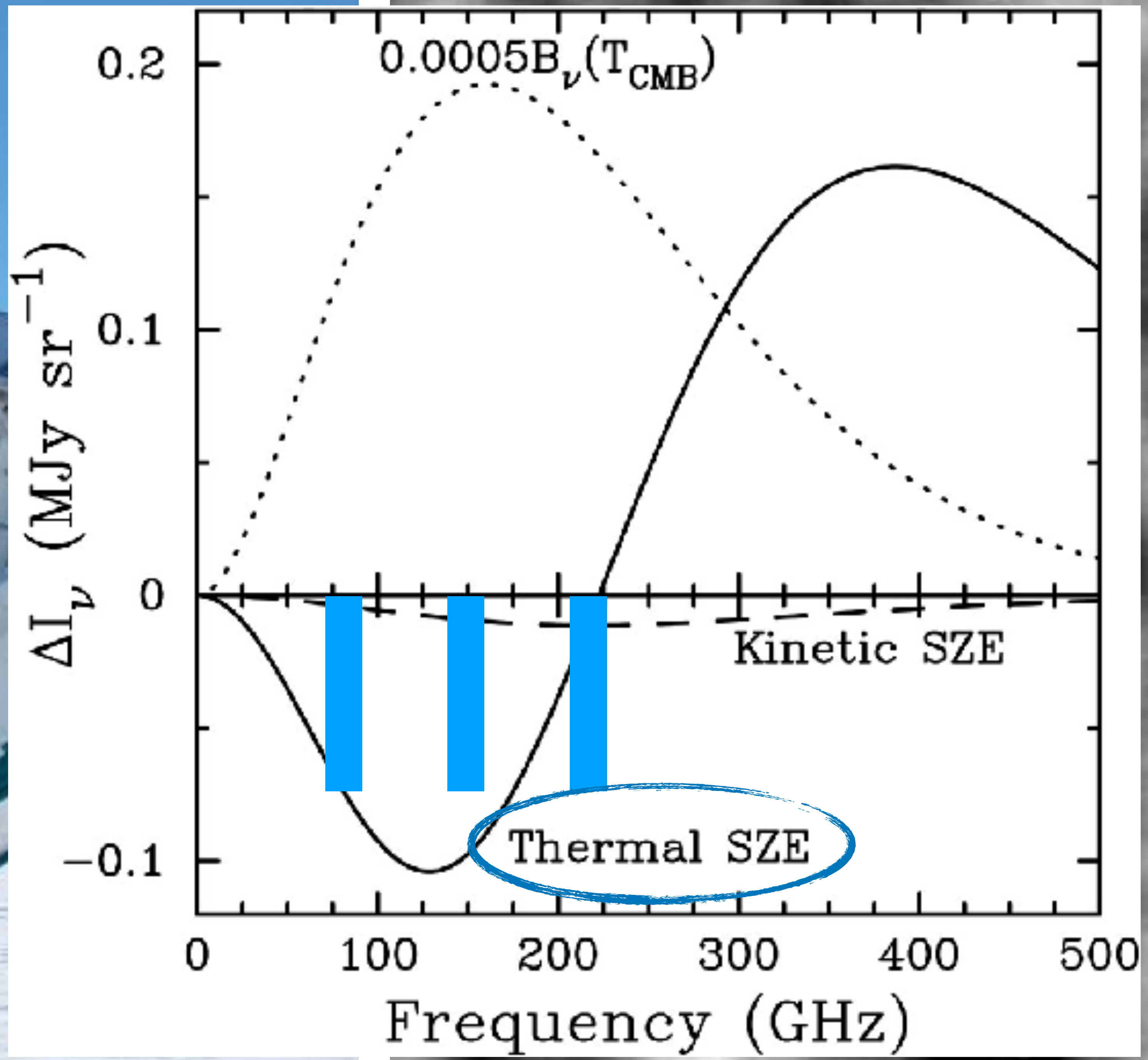

SZ spectrum

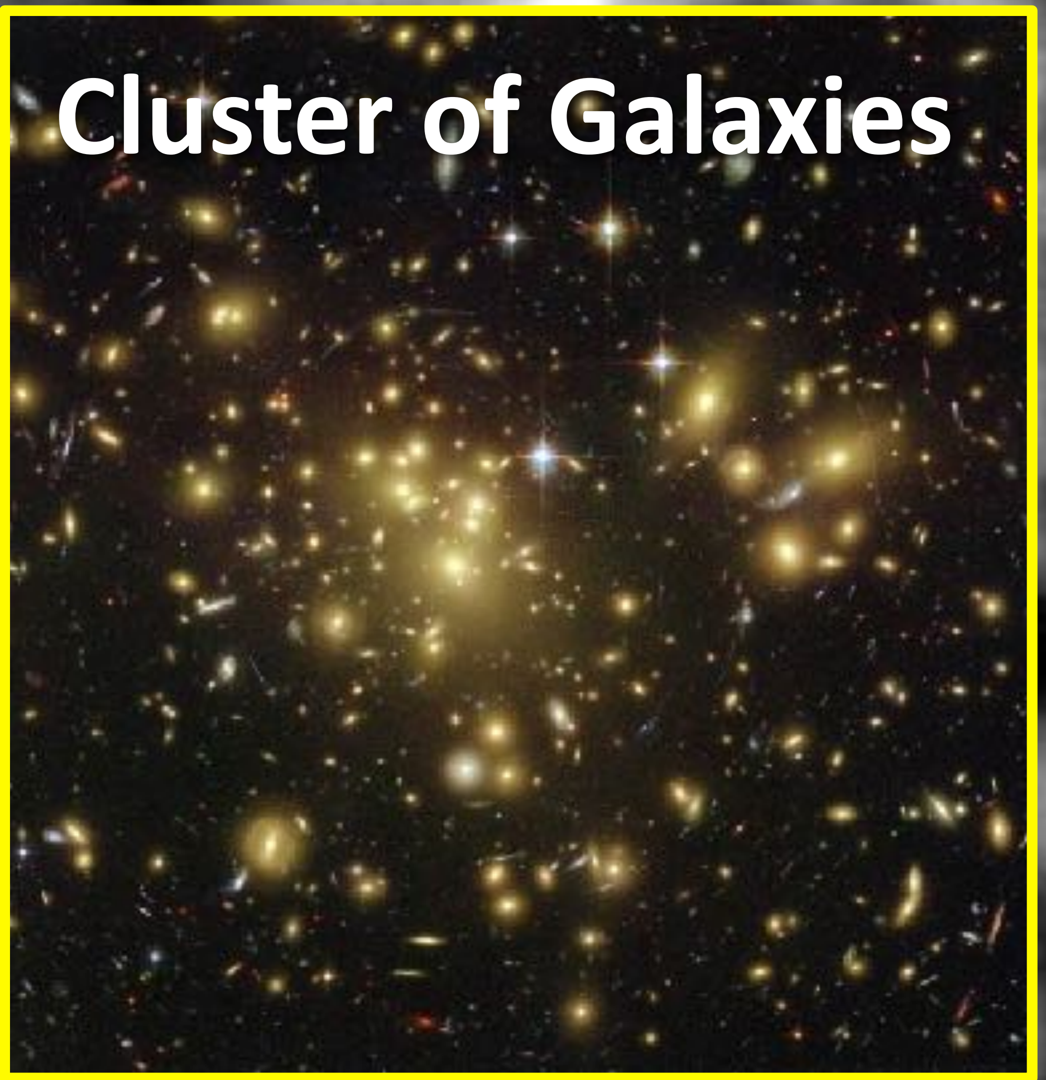

Clean and well-understood selection of cluster candidates

Out to highest redshifts where clusters exist!

SPTpol @ 150 GHz

Why use SZ-selected clusters?

Three approaches: X-ray, Optical, SZ

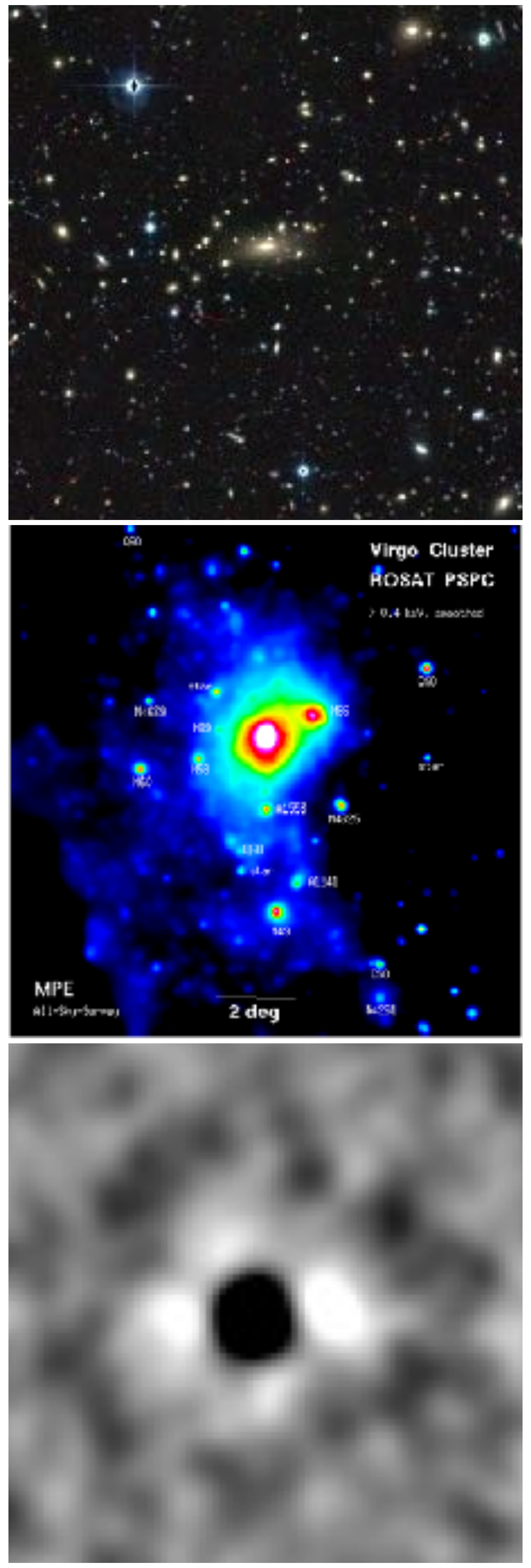

Weinberg et al. 2013

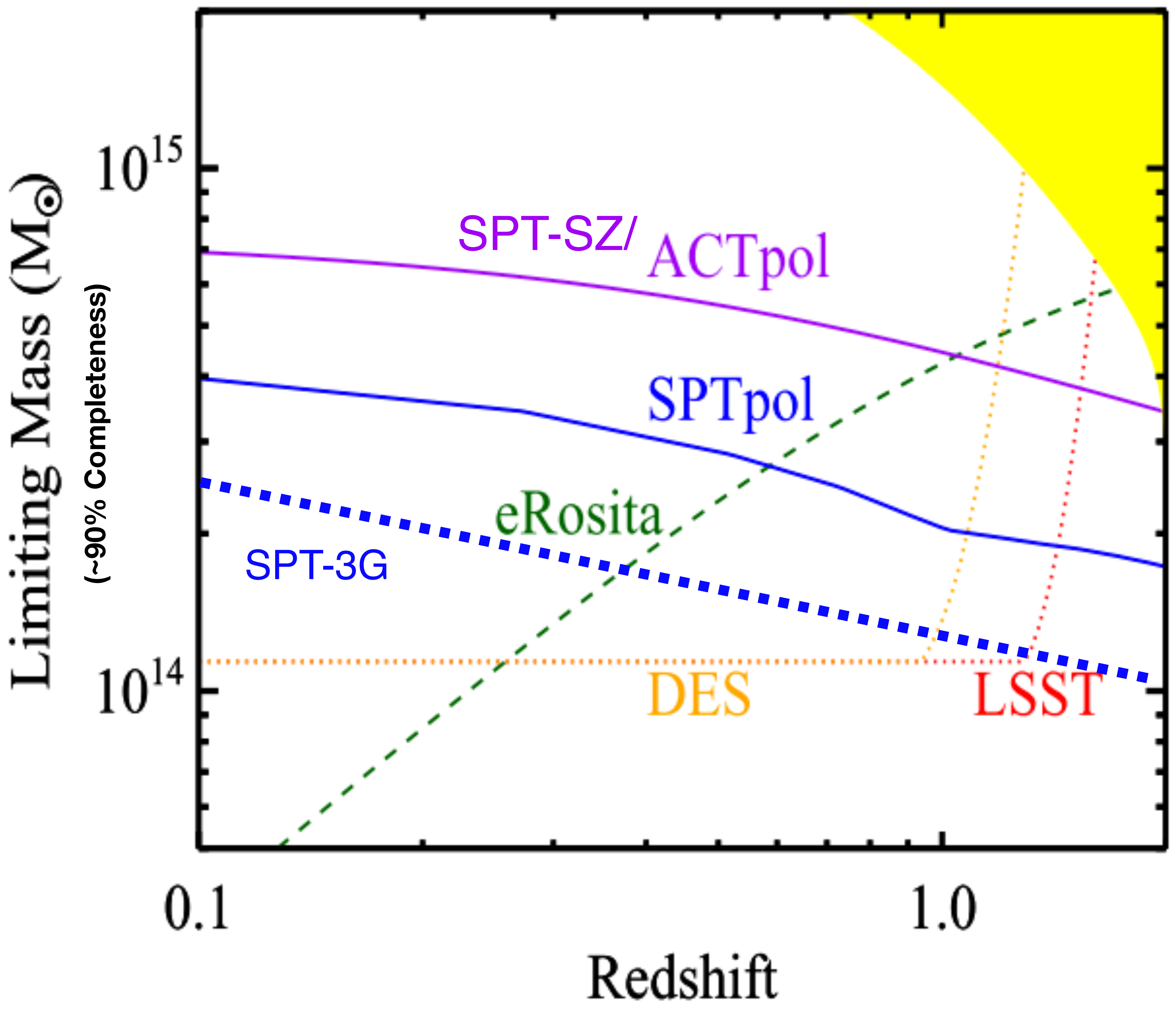

SZ: clean, well-understood selection

Complementarity with other methods

Kéruzoré et al. 2023

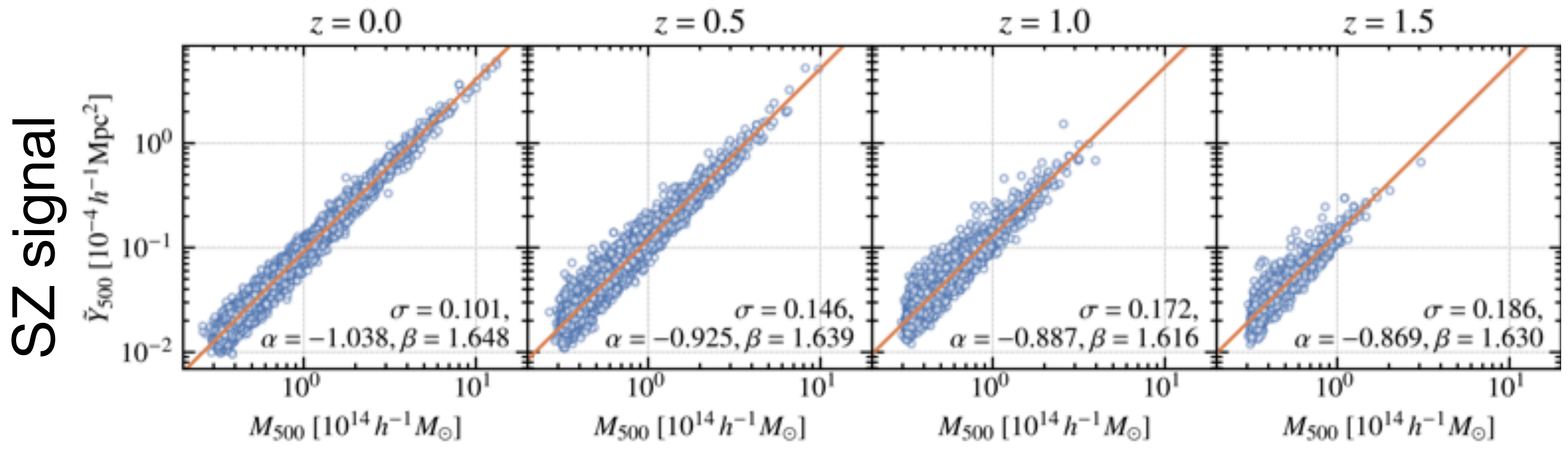

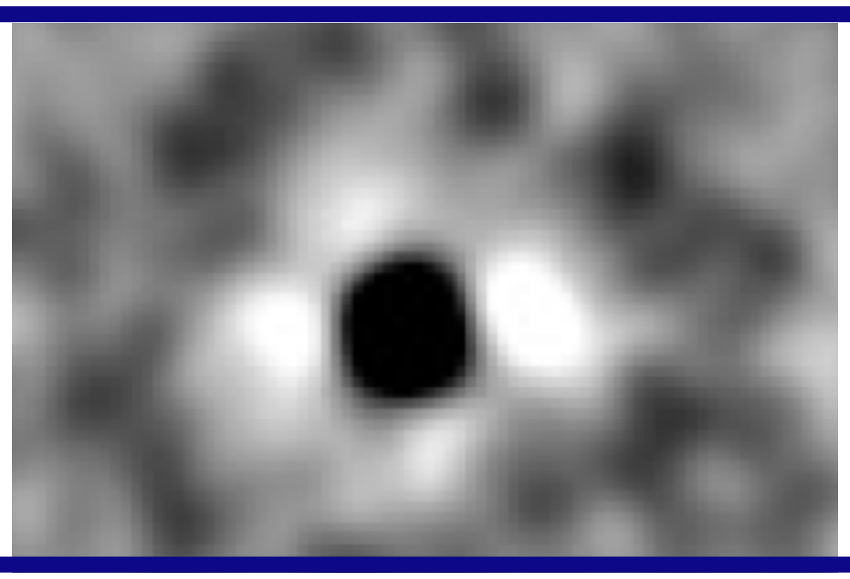

How to confirm SZ candidates?

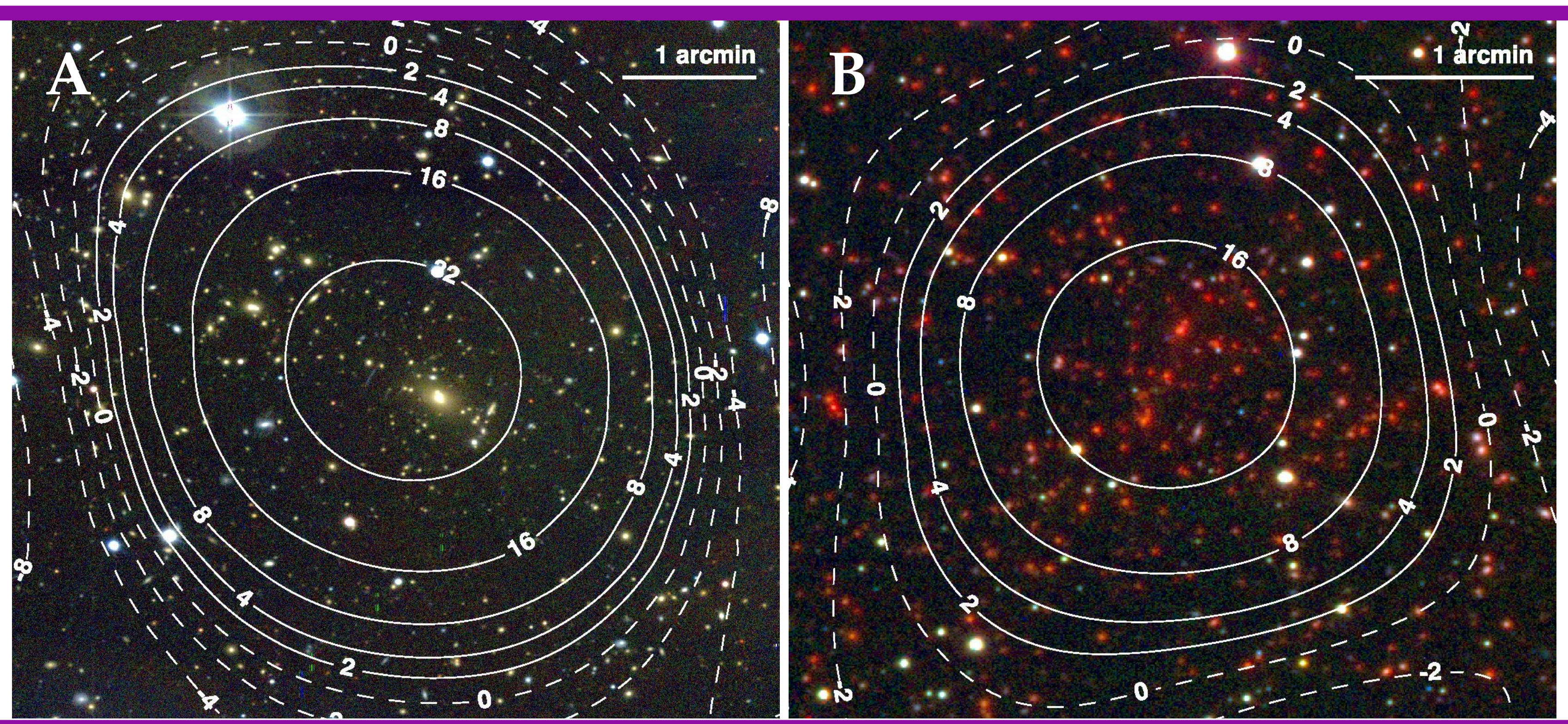

Measure richness (≅number of cluster member galaxies) and redshift

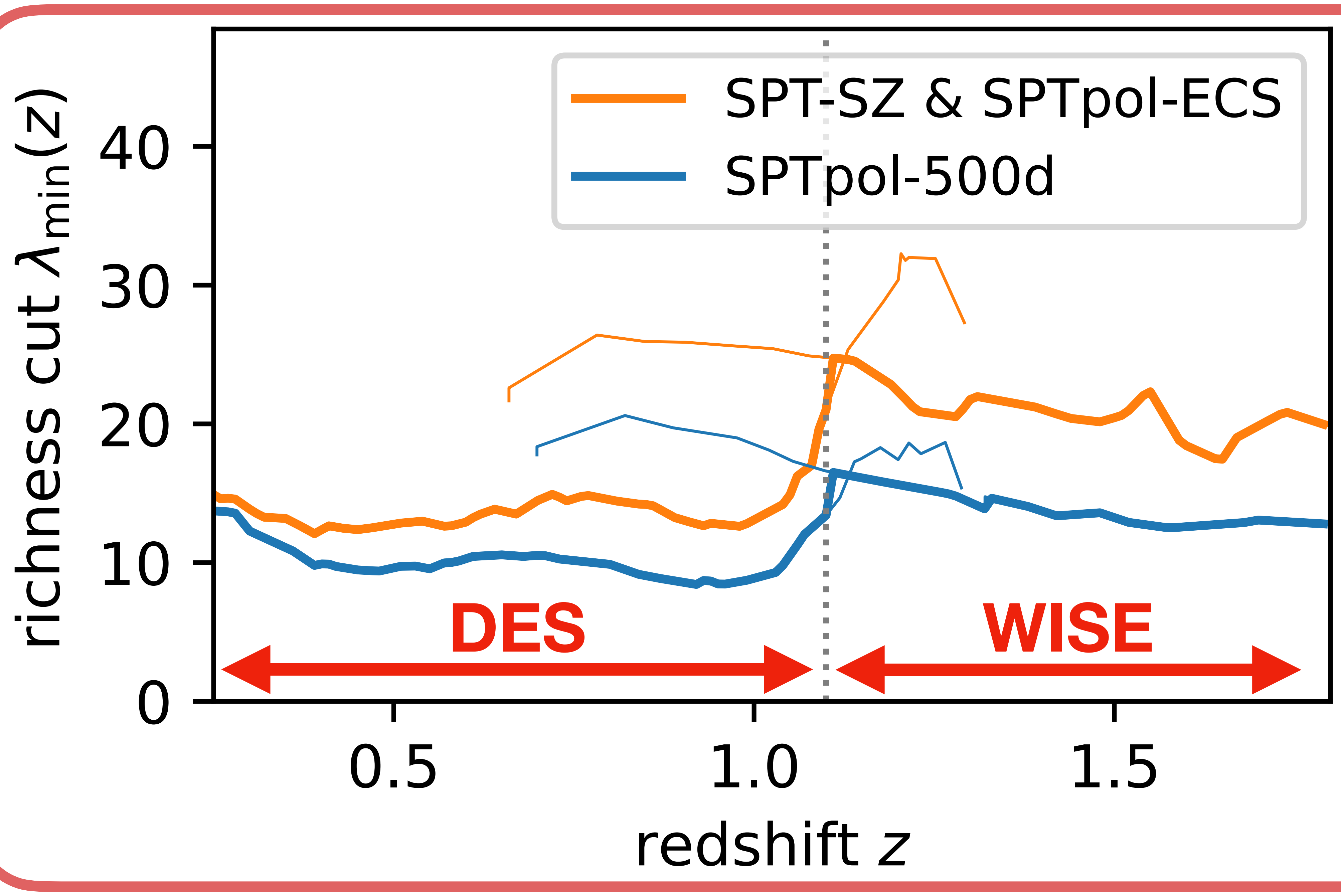

Get rid of chance associations (with SPT noise fluctuation)

Calibrate probability of chance association by measuring (λ, z) at random locations

Establish $\lambda_{min}(z)$ to achieve target purity (> 98%)

(Klein+18,23; Bleem+24)

The Dark Energy Survey

5000 deg^2 galaxies & weak lensing

Catalog of SPT-selected cluster candidates needs

- Confirmation
- Cluster redshifts
- Weak-lensing (mass) measurement

all of which DES was designed for

(here we use DES Year 3 data = Y3)

Image credit: CTIO/NOIRLab/NSF/AURA/D. Munizaga

SPT(SZ+pol) Cluster Sample

1,005 confirmed clusters above *z* > 0.25 over 5,200 deg²

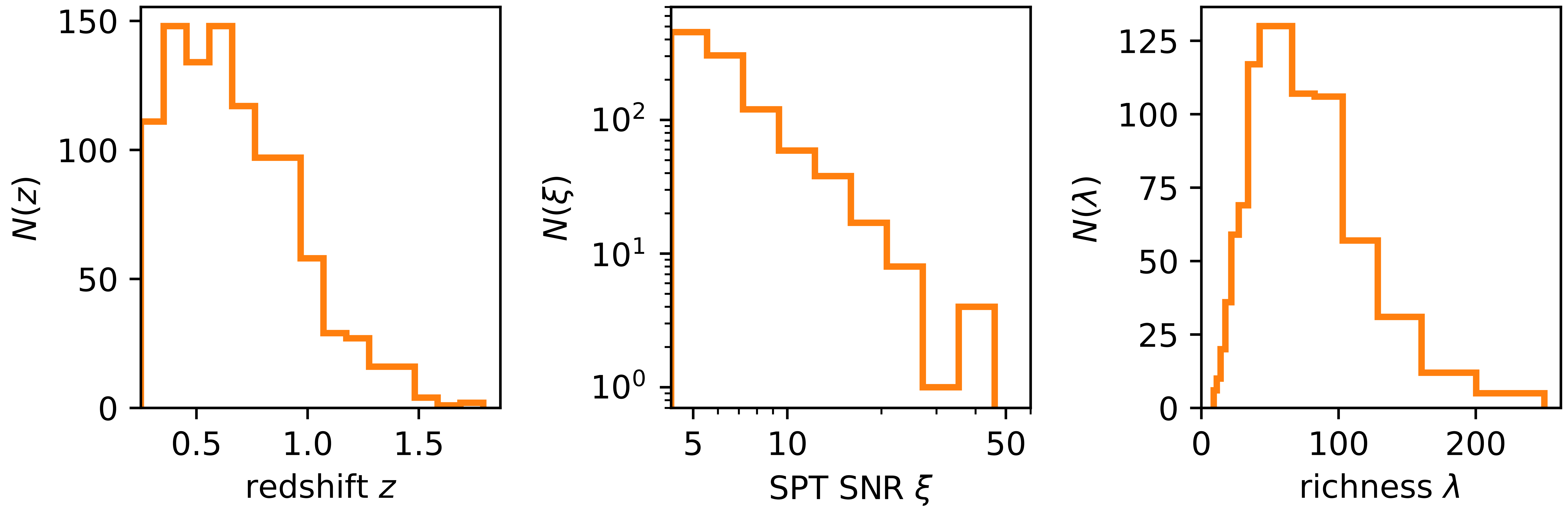

SPT Clusters and the Dark Energy Survey

3,600 deg² overlap

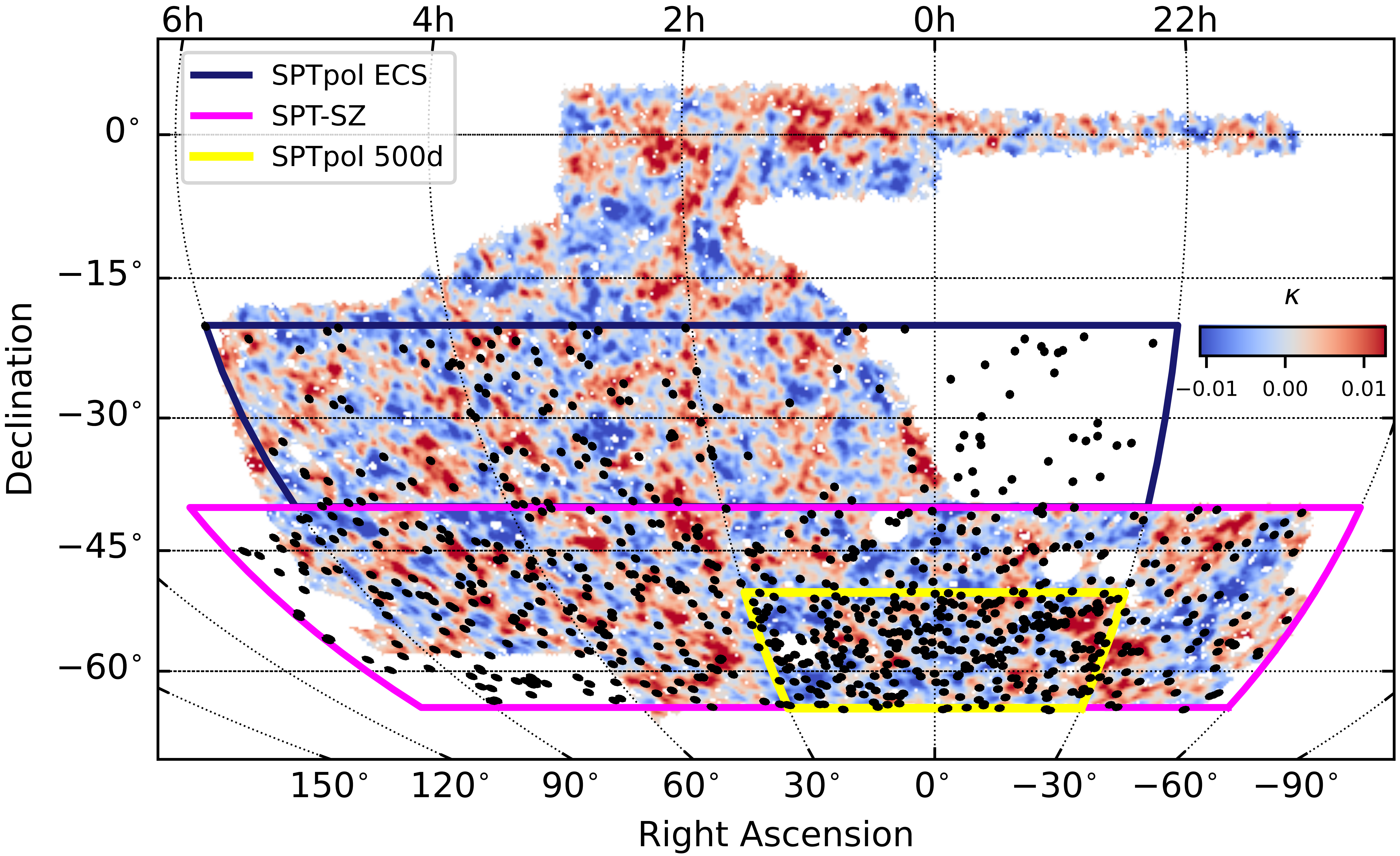

Bleem+15,20,24
Klein+24
Bocquet+24II

Cluster lensing analysis
Shear profiles

- Almost 700 SPT clusters (redshift 0.25—0.95) with DES Y3 shear
    - For the experts:
        - Analysis uses individual cluster shear profiles (Stacks are shown for visualization purposes)
        - Same source selection as in DES Y3 3x2pt
            - Same photo-*z* and shear calibrations
        - Radial range: $0.5 < r\ [h^{-1}\mathrm{Mpc}] < 3.2 / (1 + z)$ (avoid cluster centers, stay in 1-halo term regime)
- 39 high-redshift clusters (redshift 0.6—1.7) with the Hubble Space Telescope
  Schrabback+18, Schrabback,Bocquet+21, Zohren,Schrabback,Bocquet+22

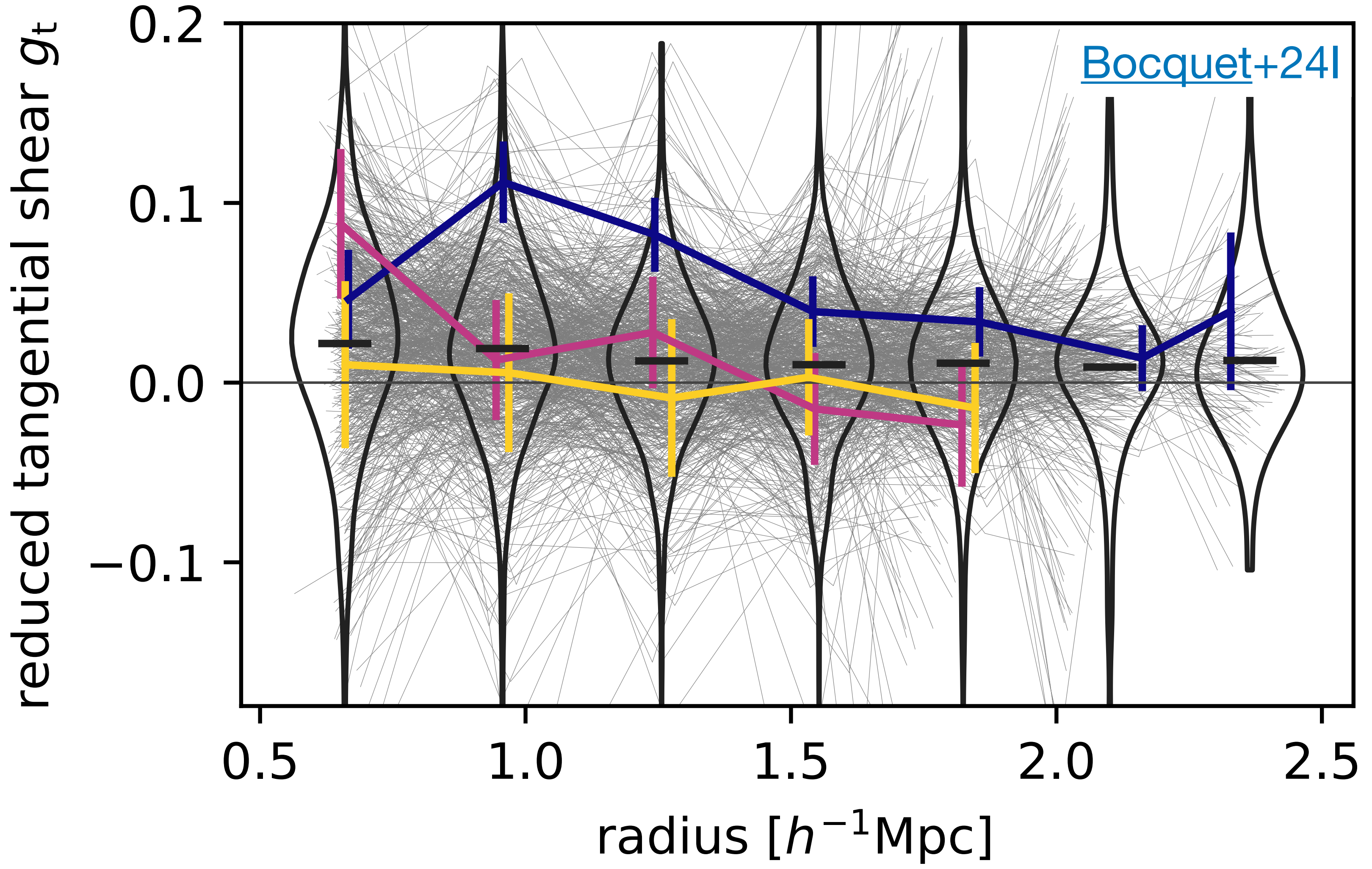

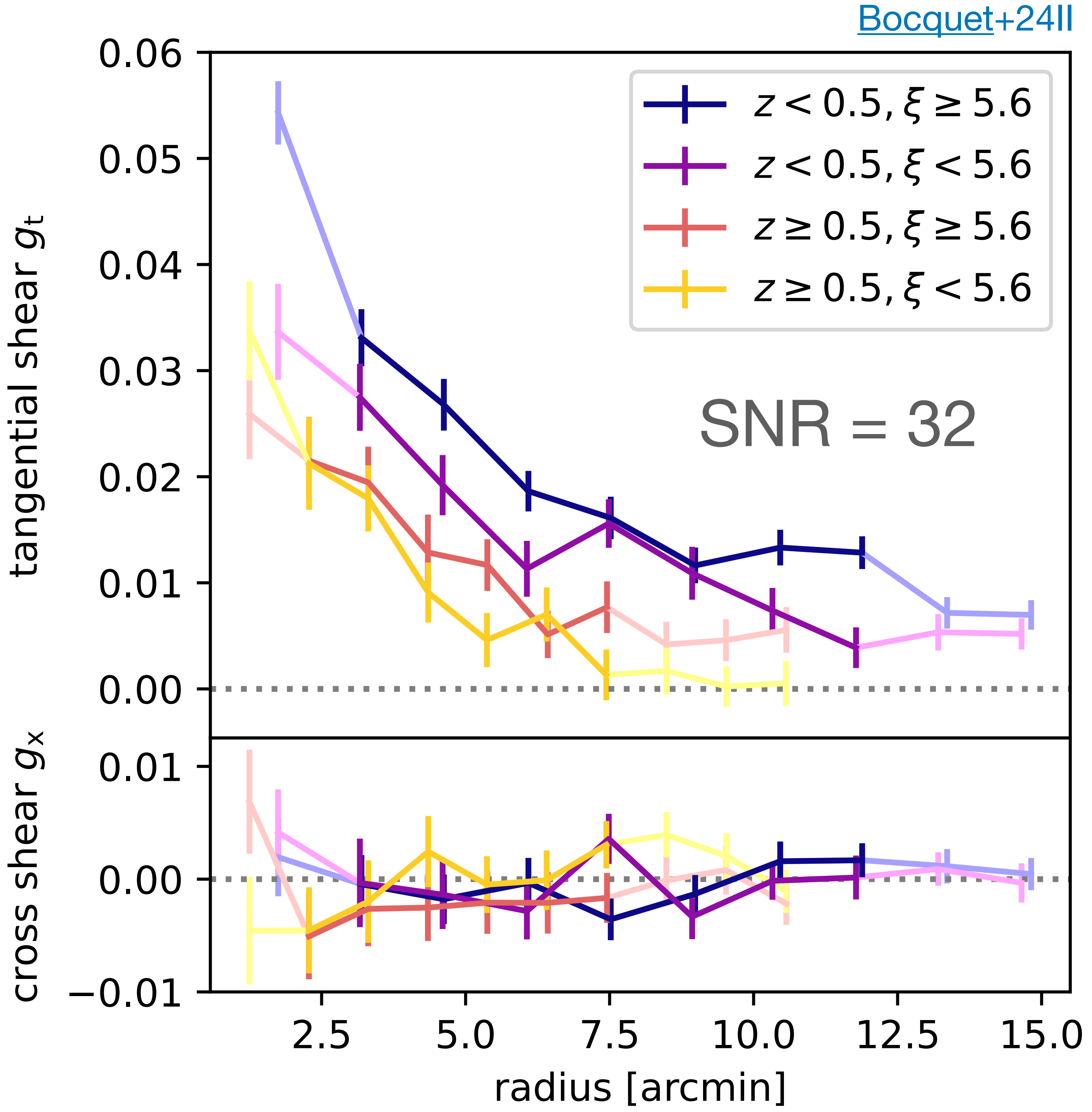

Likelihood Function I

Bayesian Population Modeling

Let us generate a cluster dataset!

cosmological: halo mass function

astrophysical: observable—mass relation

observational: telescope, detector, atmosphere, etc.

$$\frac{d^3N(\boldsymbol{p})}{dM\,dz\,dV}\,\frac{dV(z,\boldsymbol{p})}{d\Omega_\mathrm{s}} \xrightarrow{\text{Poisson draw}} \{M, z\} \xrightarrow{\text{OMR + scatter}} \{\zeta, \lambda, M_\mathrm{WL}, z\} \xrightarrow{\text{measurement noise}} \{\xi, \lambda, \boldsymbol{g}_\mathrm{t}, z\}$$

Differential multi-observable cluster abundance

$$\frac{d^4N(\boldsymbol{p})}{d\xi\,d\lambda\,d\boldsymbol{g}_\mathrm{t}\,dz} = \int\ldots\int dM\,d\zeta\,d\tilde{\lambda}\,dM_\mathrm{WL}\,d\Omega_\mathrm{s}\,P(\xi\,|\,\zeta)P(\lambda\,|\,\tilde{\lambda})P(\boldsymbol{g}_\mathrm{t}\,|\,M_\mathrm{WL})P(\zeta,\lambda,M_\mathrm{WL}\,|\,M,z,\boldsymbol{p})\frac{d^2N(\boldsymbol{p})}{dM\,dV}\,\frac{d^2V(z,\boldsymbol{p})}{dz\,d\Omega_\mathrm{s}}$$

marginalize over latent variables

Likelihood Function II

Poisson likelihood function: $\mathscr{L}(k\ \textbf{events} \mid \textbf{rate}\ \mu) \propto \mu^k e^{-\mu} \Rightarrow \ln \mathscr{L} = k \ln(\mu) - \mu$

$$\ln \mathscr{L}(\boldsymbol{p}) = \sum_i \ln \left. \frac{d^4 N(\boldsymbol{p})}{d\xi\, d\lambda\, d\boldsymbol{g}_\mathrm{t}\, dz} \right|_{\xi_i, \lambda_i, g_{\mathrm{t},i}, z_i} - \int \dots \int d\xi\, d\lambda\, d\boldsymbol{g}_\mathrm{t}\, dz\, \frac{d^4 N(\boldsymbol{p})}{d\xi\, d\lambda\, d\boldsymbol{g}_\mathrm{t}\, dz} \Theta_\mathrm{s}(\xi, \lambda, z) + \mathrm{const}\,.$$

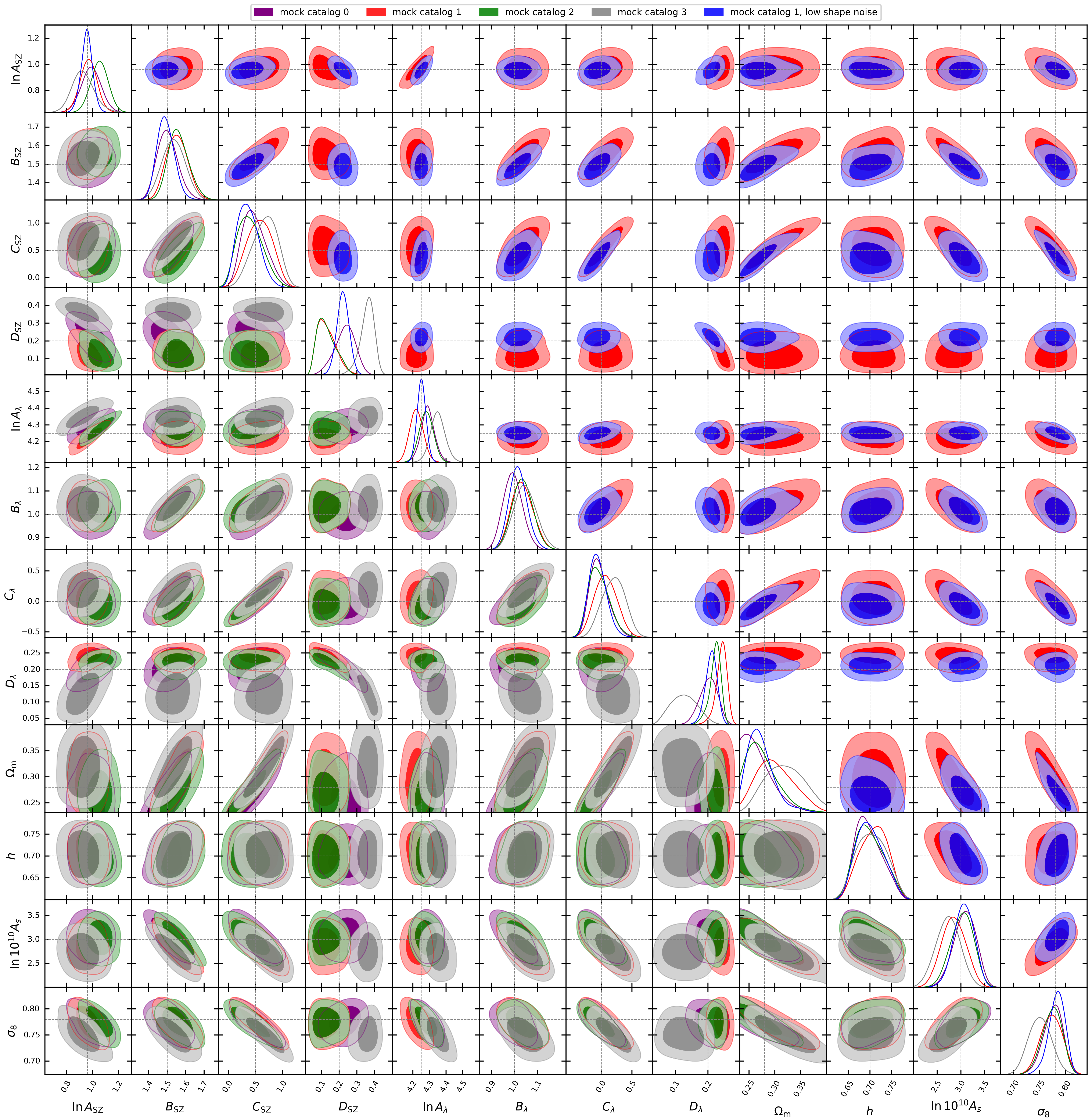

Bocquet+24I

Pipeline Verification

using mock datasets created from the model

- Create synthetic clusters from the halo mass function using observable—mass relations
- Analyze several statistically independent mock realizations
- Pipeline recovers input values
- We correctly implemented the analysis framework!

Robustness Tests during Blind Analysis Phase

All chains were blinded by applying the same unknown parameter offset

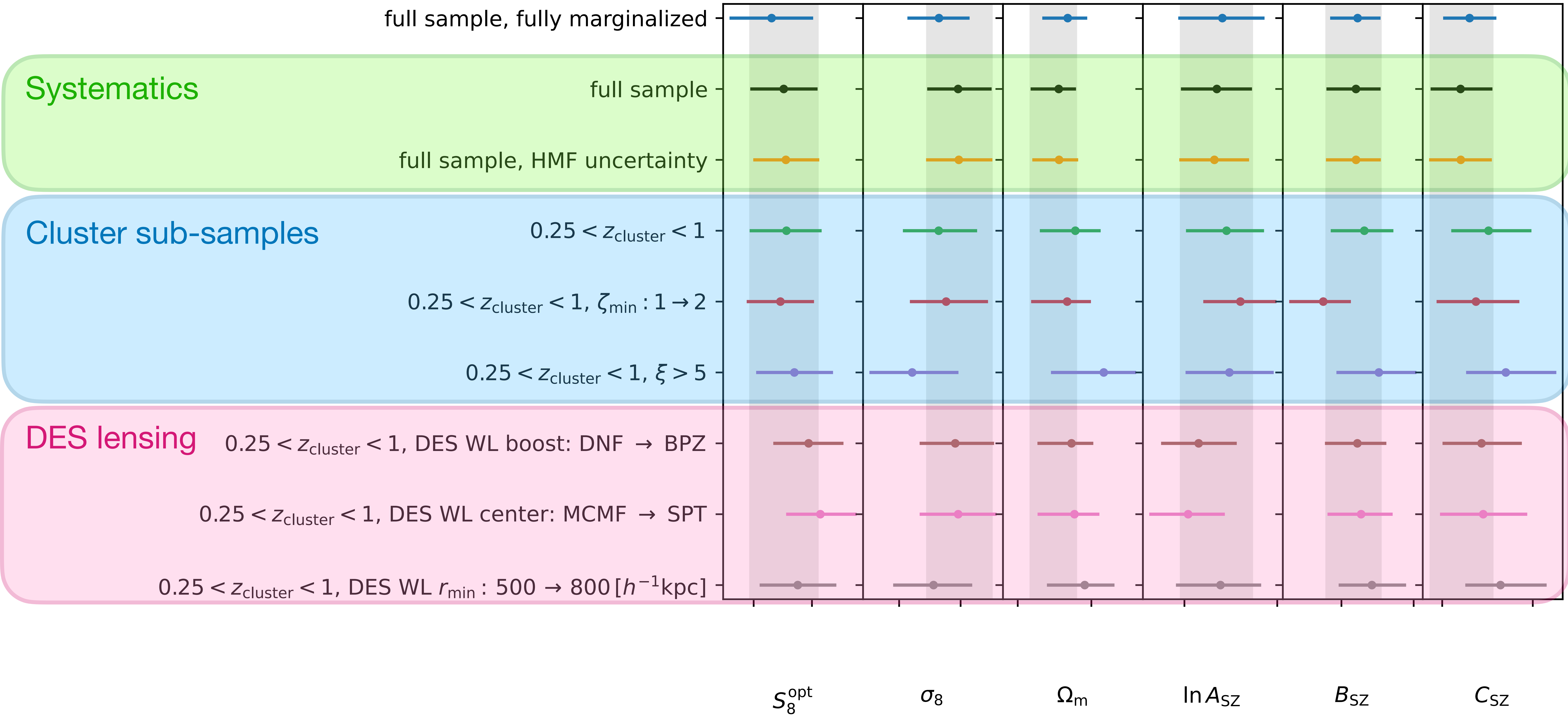

Bocquet+24II

Does the model describe the data?

Binned and stacked data for visualization

Bocquet+24II

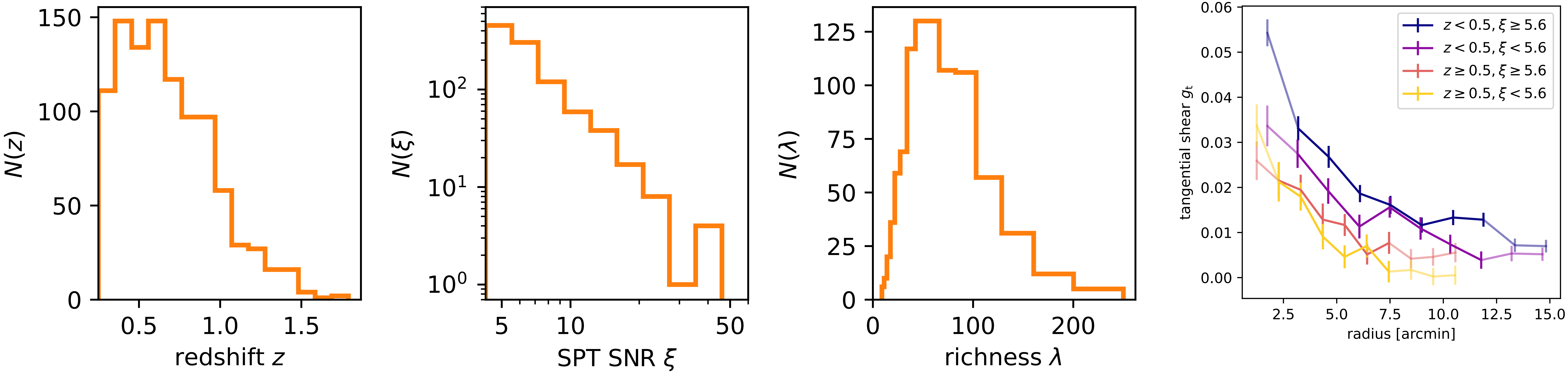

Mean recovered model (and uncertainties) from full analysis.
No significant signs of problems.

ΛCDM with massive neutrinos

Bocquet+24II

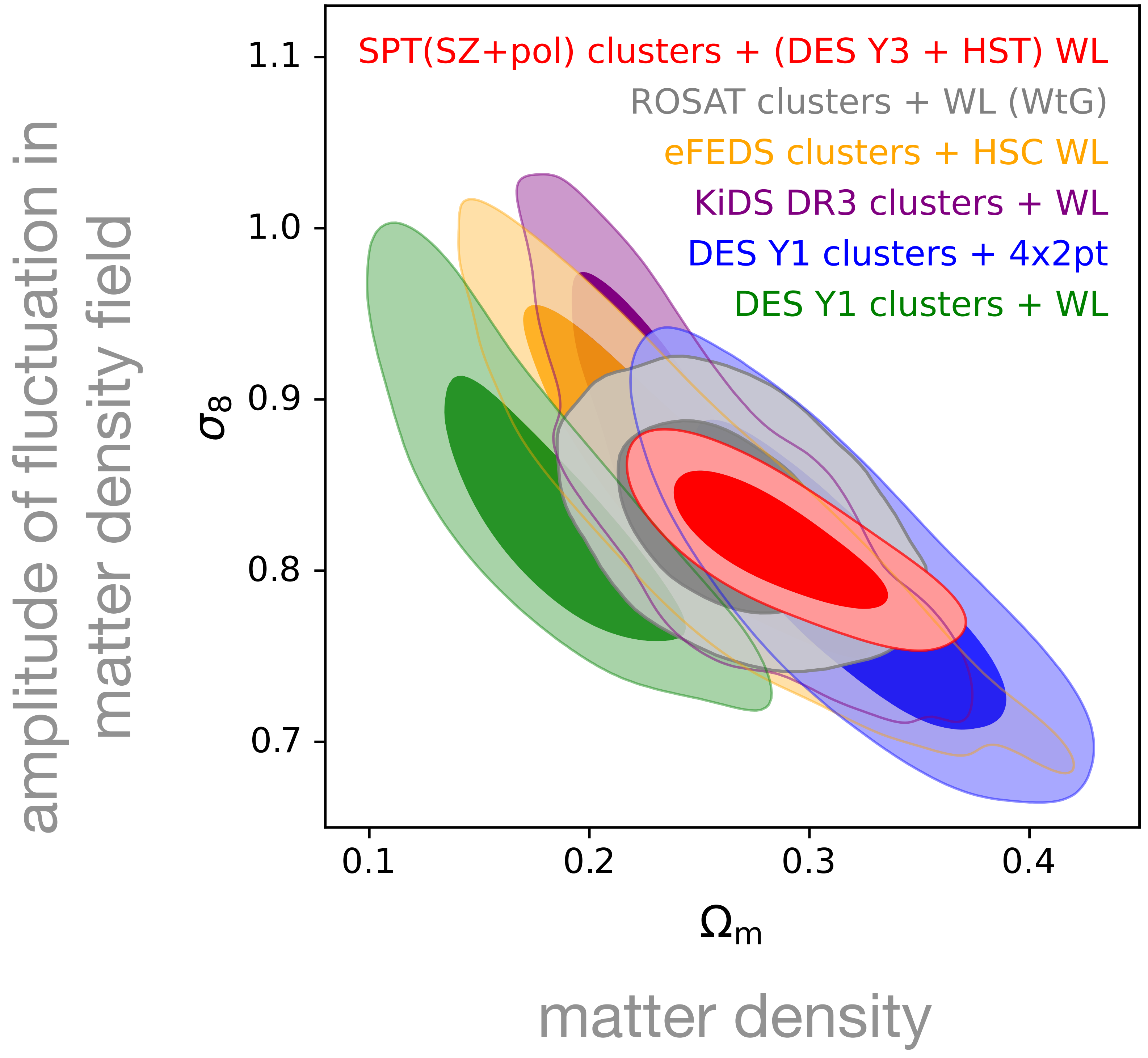

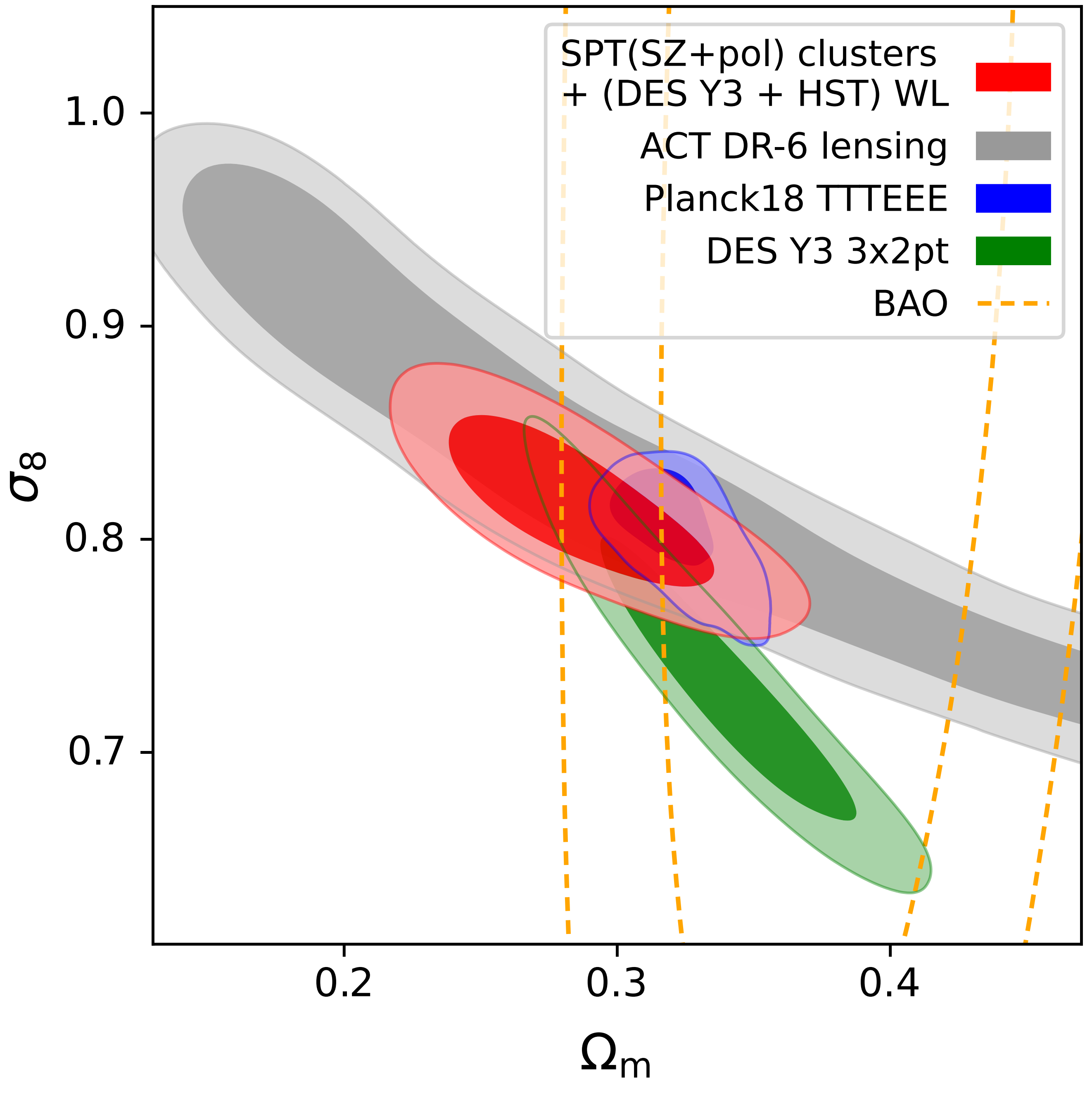

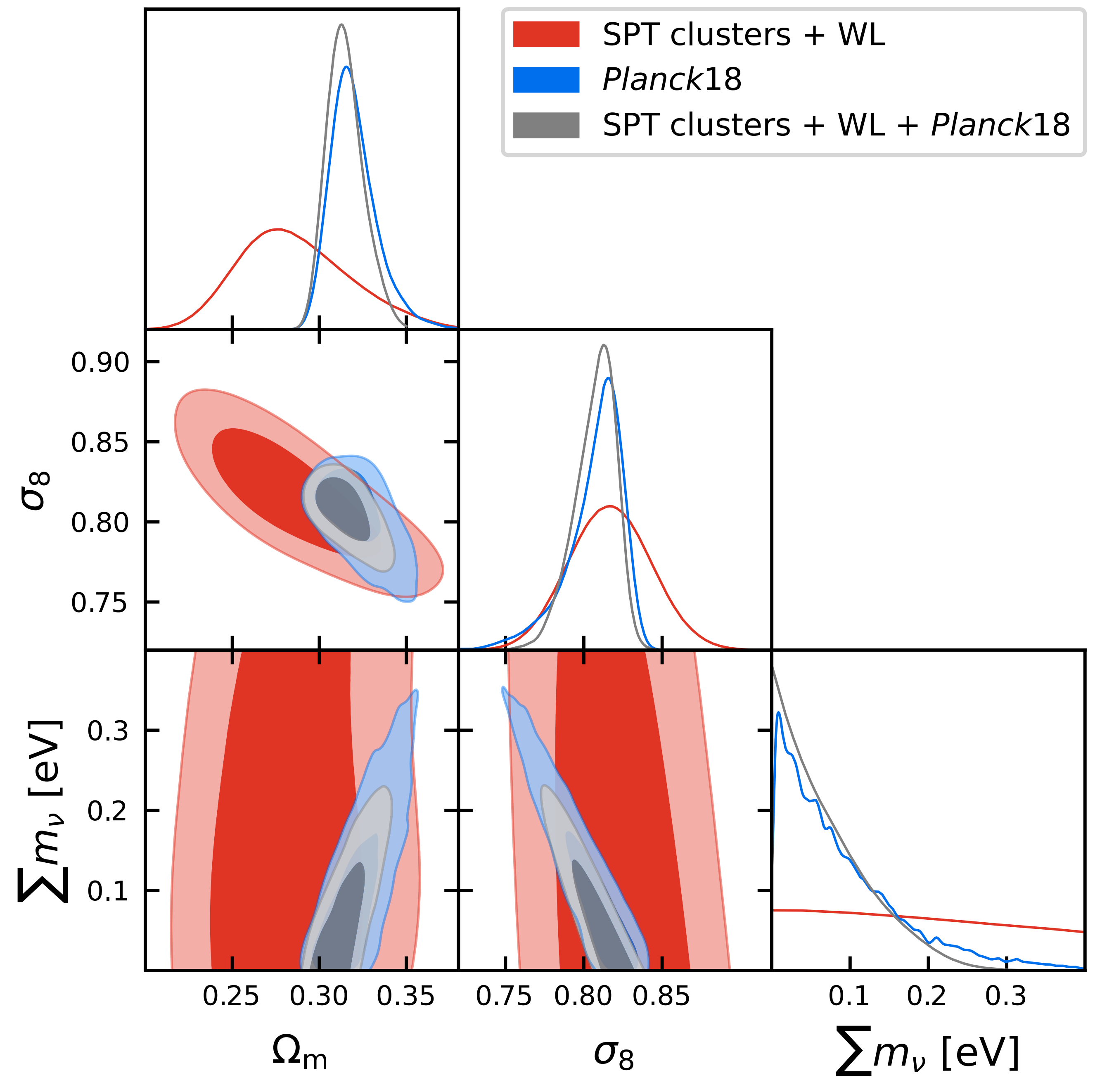

- Competitive constraints, especially on $S_8^{\rm opt} \equiv \sigma_8 \left(\Omega_{\rm m}/0.3\right)^{0.25}$
- No evidence for "S_8 tension" with Planck (1.1 σ)
- In combination with Planck $\sum m_\nu < 0.18\,{\rm eV}\,(95\,\%\,{\rm C.L.})$

Tracing the Growth of Structure

Phenomenological test

- Five bins in redshift with equal number of clusters
- Fit for independent amplitudes $\sigma_8(z)$
- With loose prior on Ω_m from the sound horizon at recombination θ_*
- Good agreement with ΛCDM model and *Planck* parameters from $z = 0.25$ to $z = 1.8$

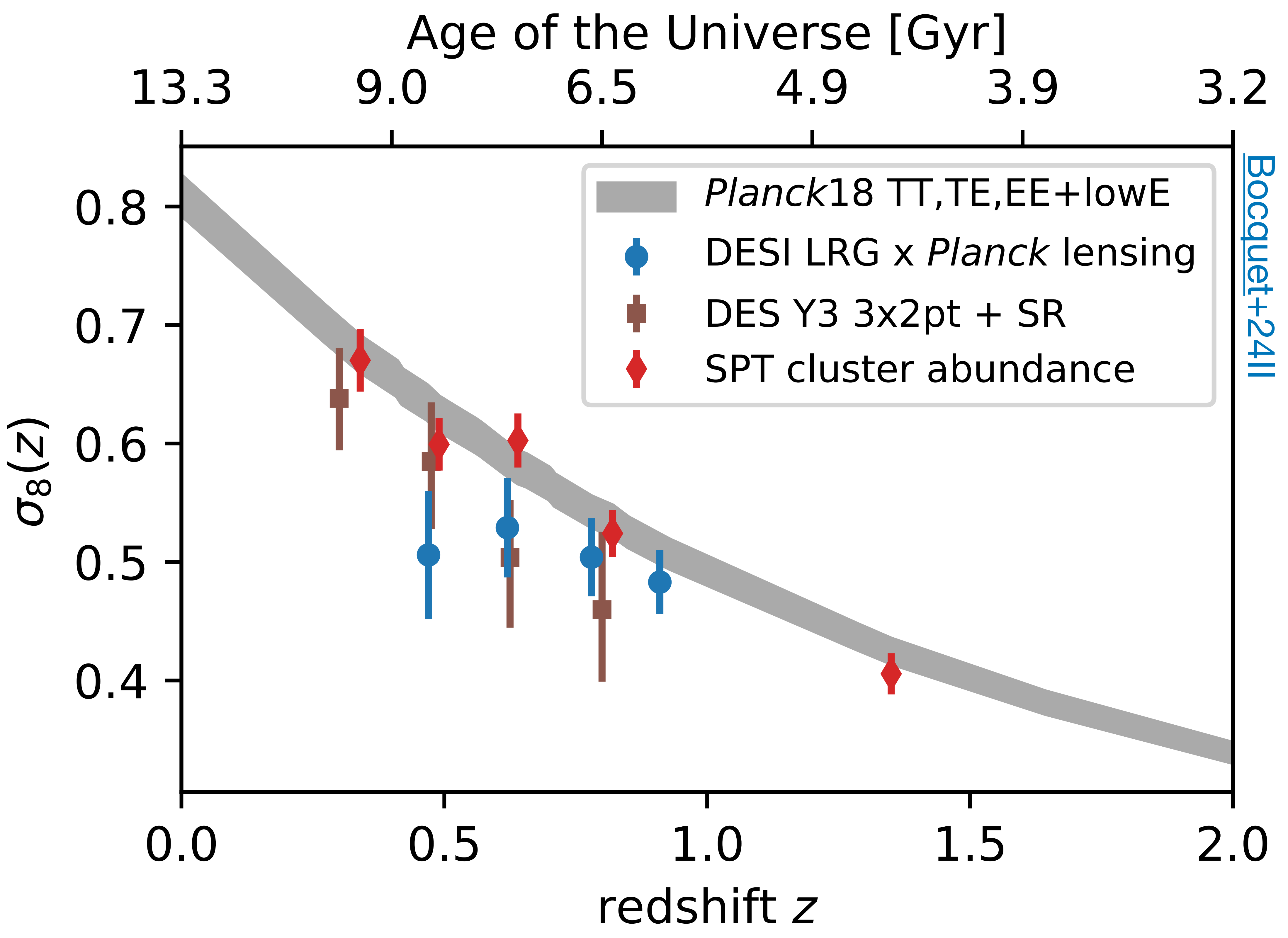

Outlook

select work by PhD students

Mazoun, Bocquet, Garny, Mohr, Rubira, Vogt 24

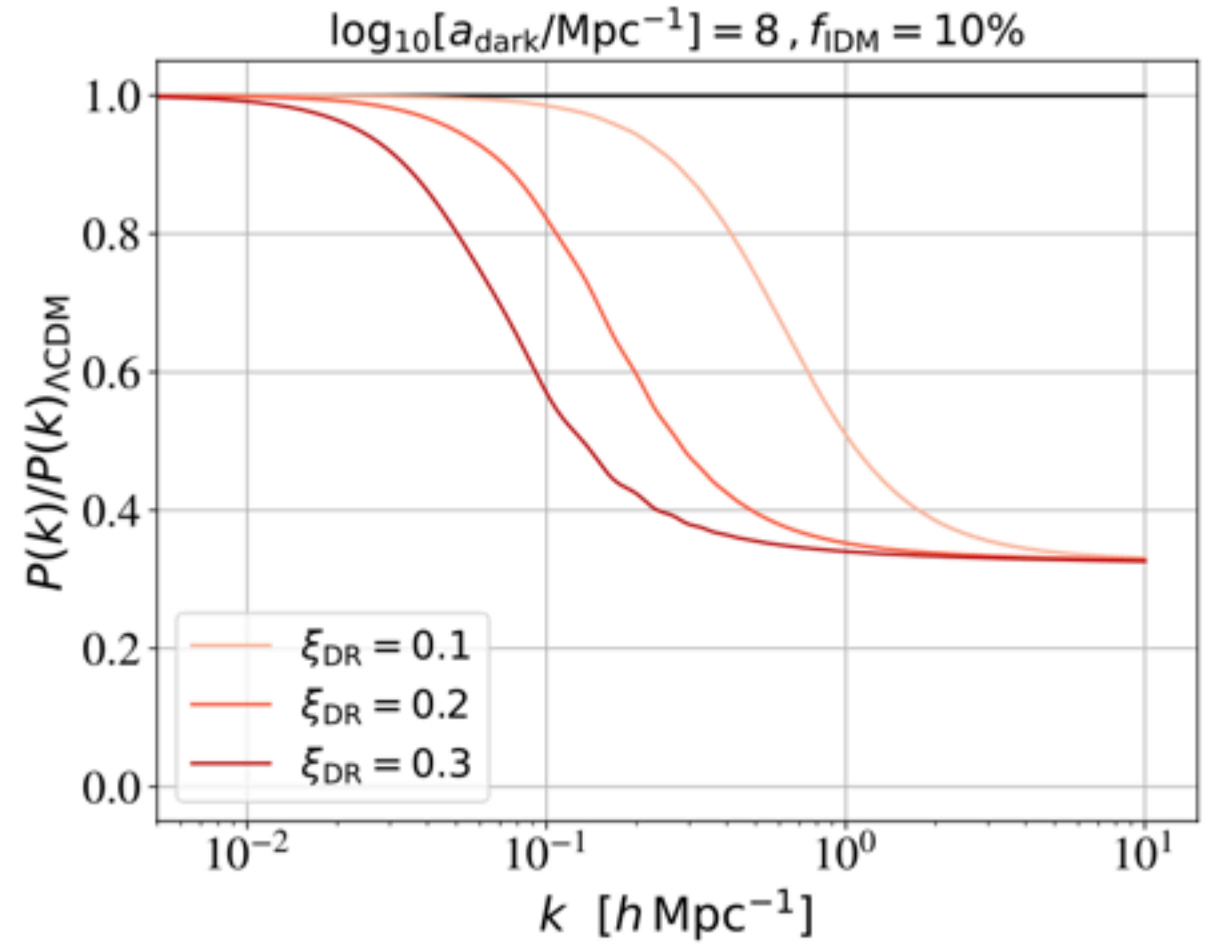

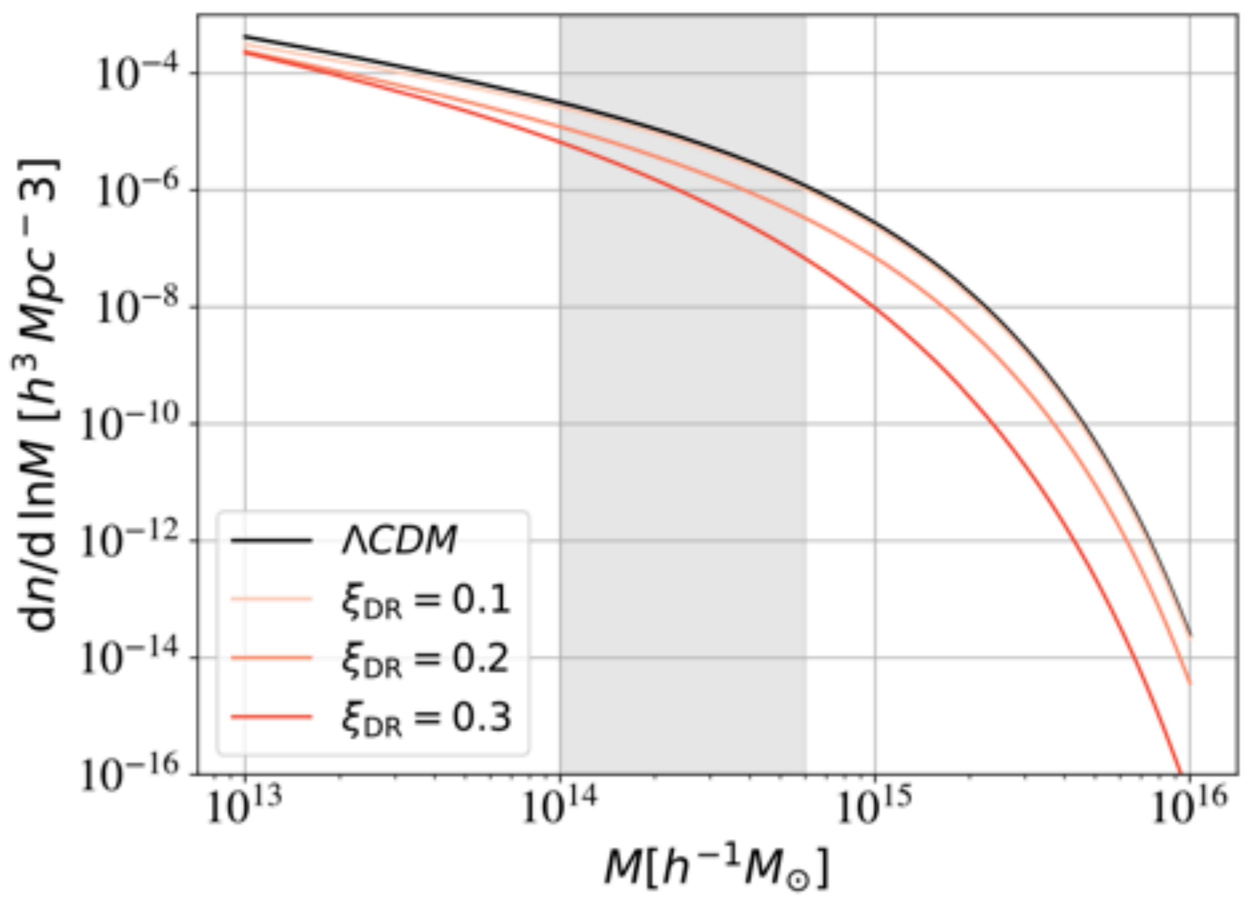

Asmaa Mazoun

Interacting dark sector models

Analysis of SPT+DES dataset ongoing
(Mazoun+ in prep.)

Sophie Vogt

f(R) and nDGP models

Analysis of SPT+DES dataset done
(Vogt+ in prep.)

Vogt, Bocquet, Davies, Mohr, Schmidt 24

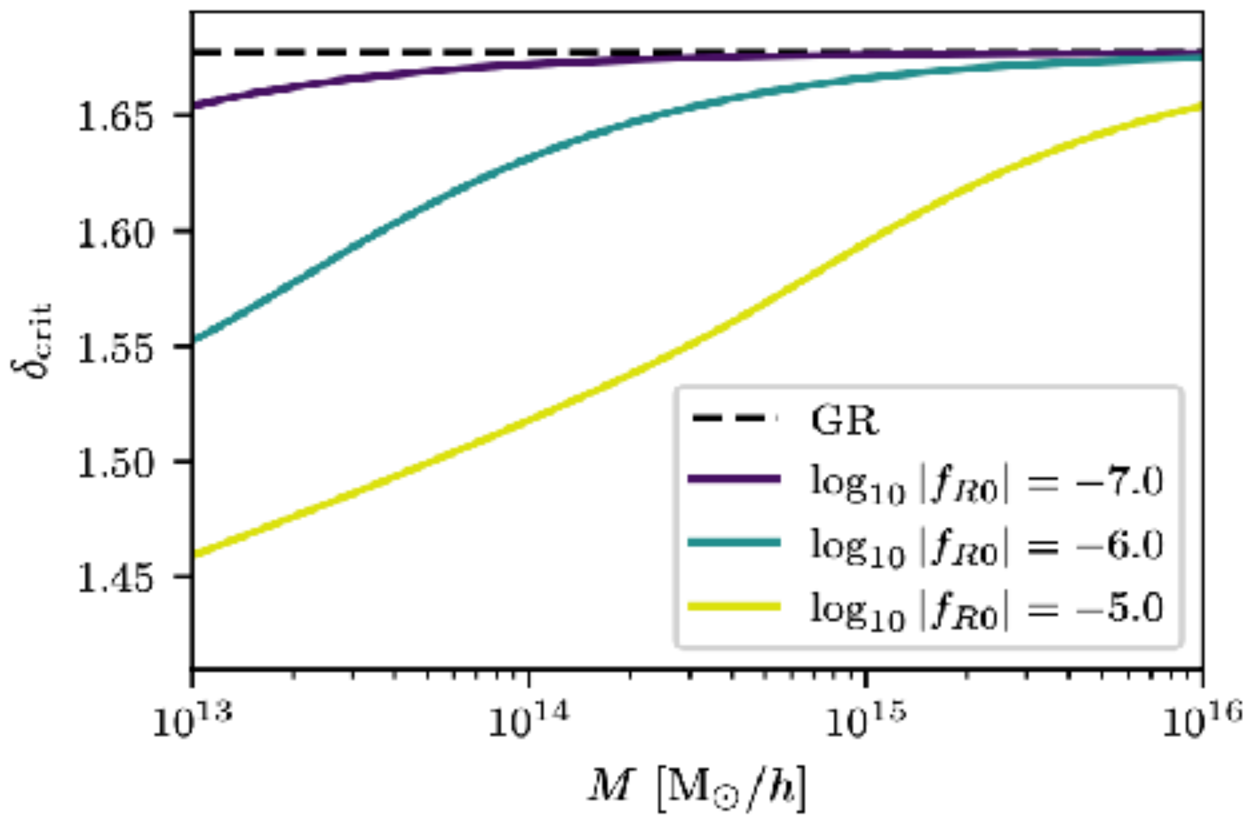

FIG. 1. The critical overdensity δ_{crit} for spherical collapse in $f(R)$ gravity (Eq. (12)) for different values of $\log_{10}|f_{R0}|$ at collapse redshift $z_c = 0$ in colored solid lines. The dashed black line represents δ_{crit} in a corresponding GR cosmology (Eq. (13)).

Outlook: Joint Constraints

SPT Cluster Abundance + DES 3x2 pt

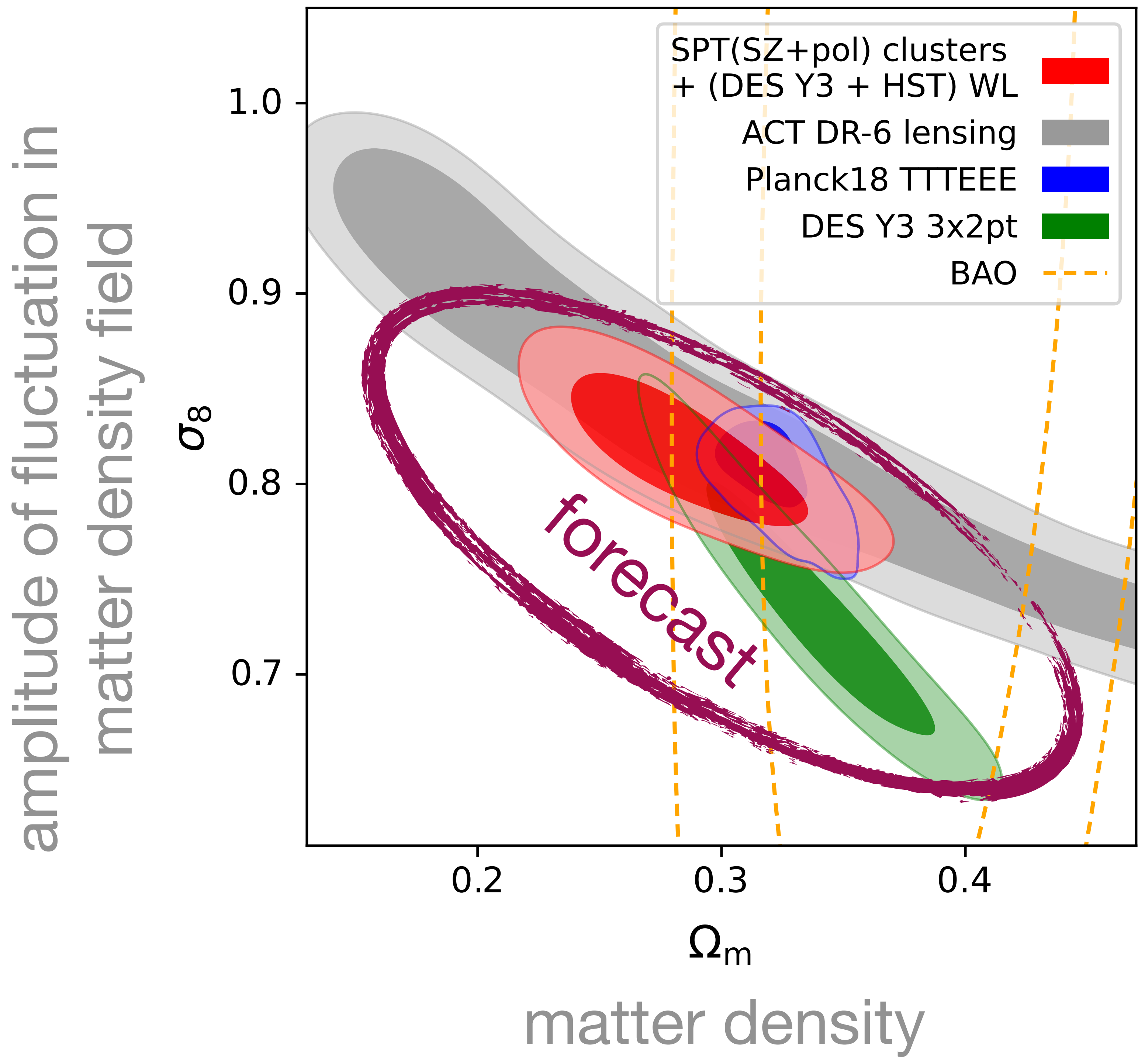

- Joint analysis
  - Cosmological covariance
  - Shared (lensing) systematics
  - Addressed w/
    Chun-Hao To, Elisabeth Krause, Sebastian Grandis
- Expect powerful constraints on $z < 2$ large-scale structure
- Ideal complement to high-redshift CMB measurements by *Planck*

The South Pole Telescope (SPT)

10-meter sub-mm quality wavelength telescope

90, 150, 220 GHz and
1.6, 1.2, 1.0 arcmin resolution

2007: SPT-SZ
960 detectors
90,150,220 GHz

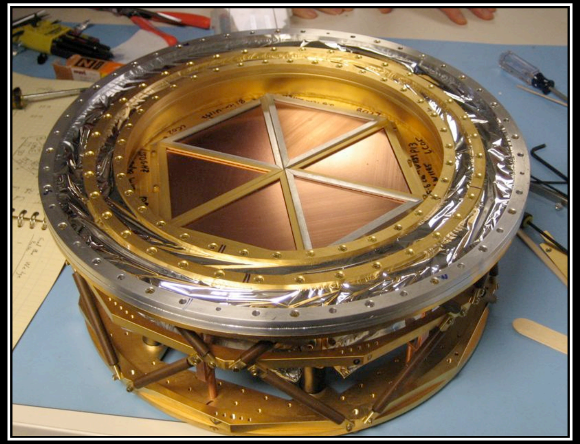

2012: SPTpol
1600 detectors
90,150 GHz
+Polarization

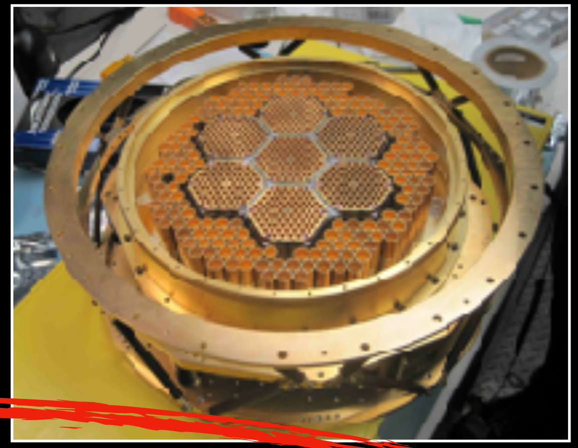

2017: SPT-3G
~15,200 detectors
90,150,220 GHz
+Polarization

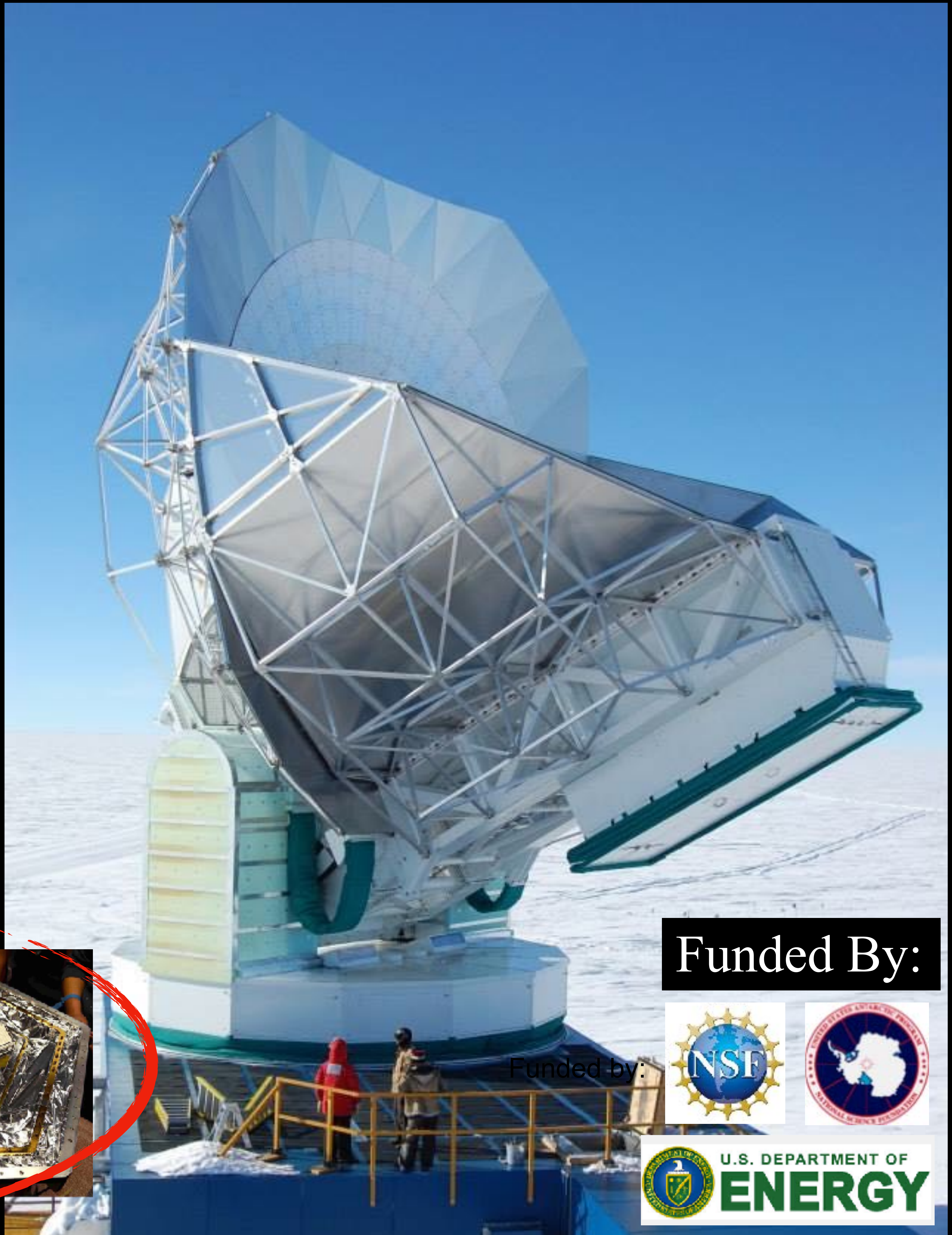

Funded By:

The 10,000 deg² SPT-3G Survey(s)

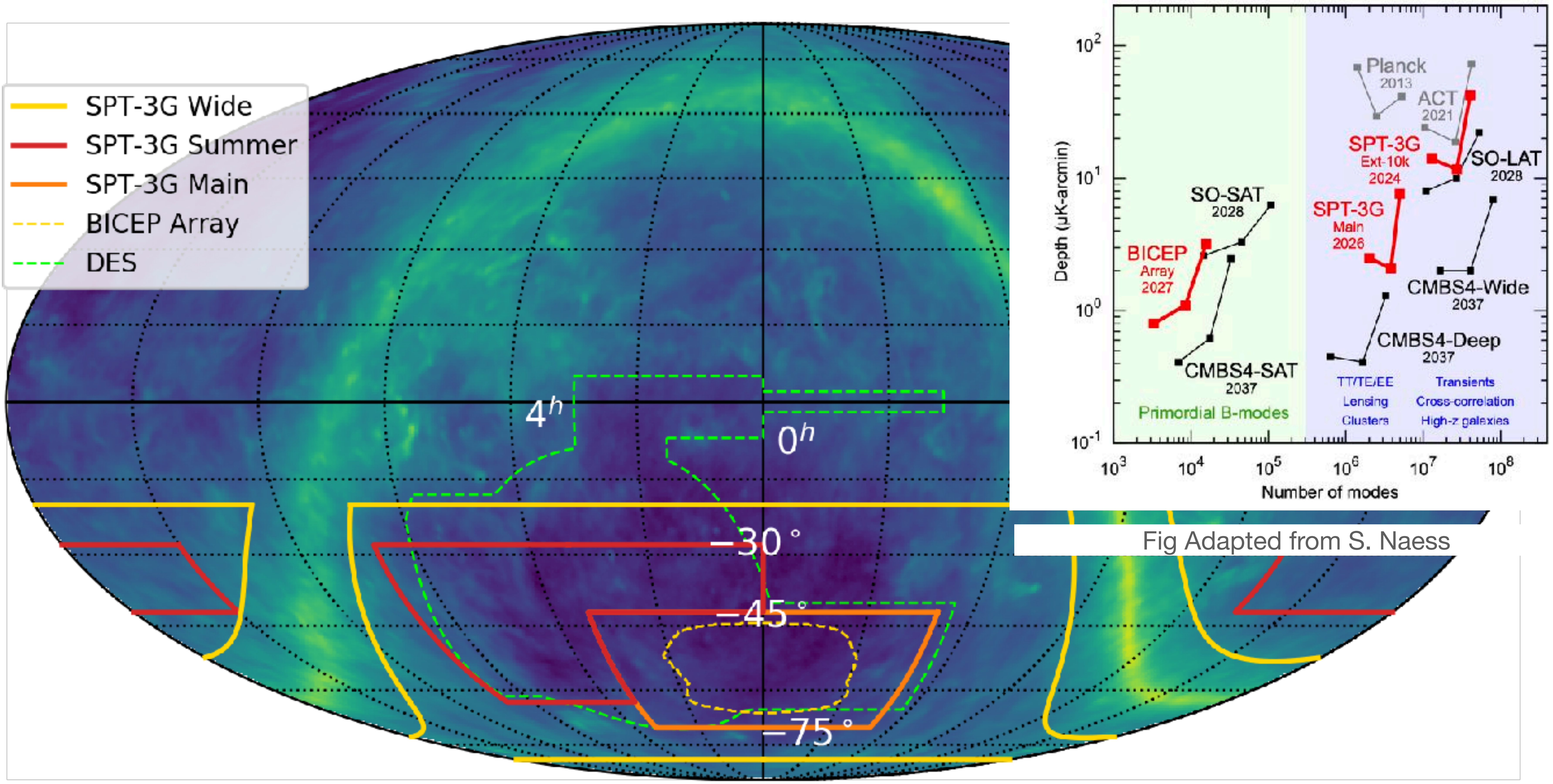

Fig Adapted from S. Naess

Survey	Area [deg^2]	Years observed	Noise level (T) [μK-arcmin]			
			95 GHz	150 GHz	220 GHz	Coadded
SPT-3G Main	1500	2019-2023, 2025-2026	2.5	2.1	7.6	1.6
SPT-3G Summer	2600	2019-2023	8.5	9.0	31	6.1
SPT-3G Wide	6000	2024	14	12	42	8.8

Wide is still 2—3 times deeper than SPT-SZ!

Slide from Lindsey Bleem

Summary

- Cluster abundance as a cosmological probe
- SZ-selection + weak-lensing mass calibration = excellent control over systematics
- Latest analysis of SPT (SZ+pol) clusters with DES Y3 + HST lensing is competitive and compatible with other probes
- Next few years will be spectacular (SPT-3G, advACT, SO, eROSITA, DES Y6, KiDS, HSC, Euclid, LSST, CMB-S4, etc.)

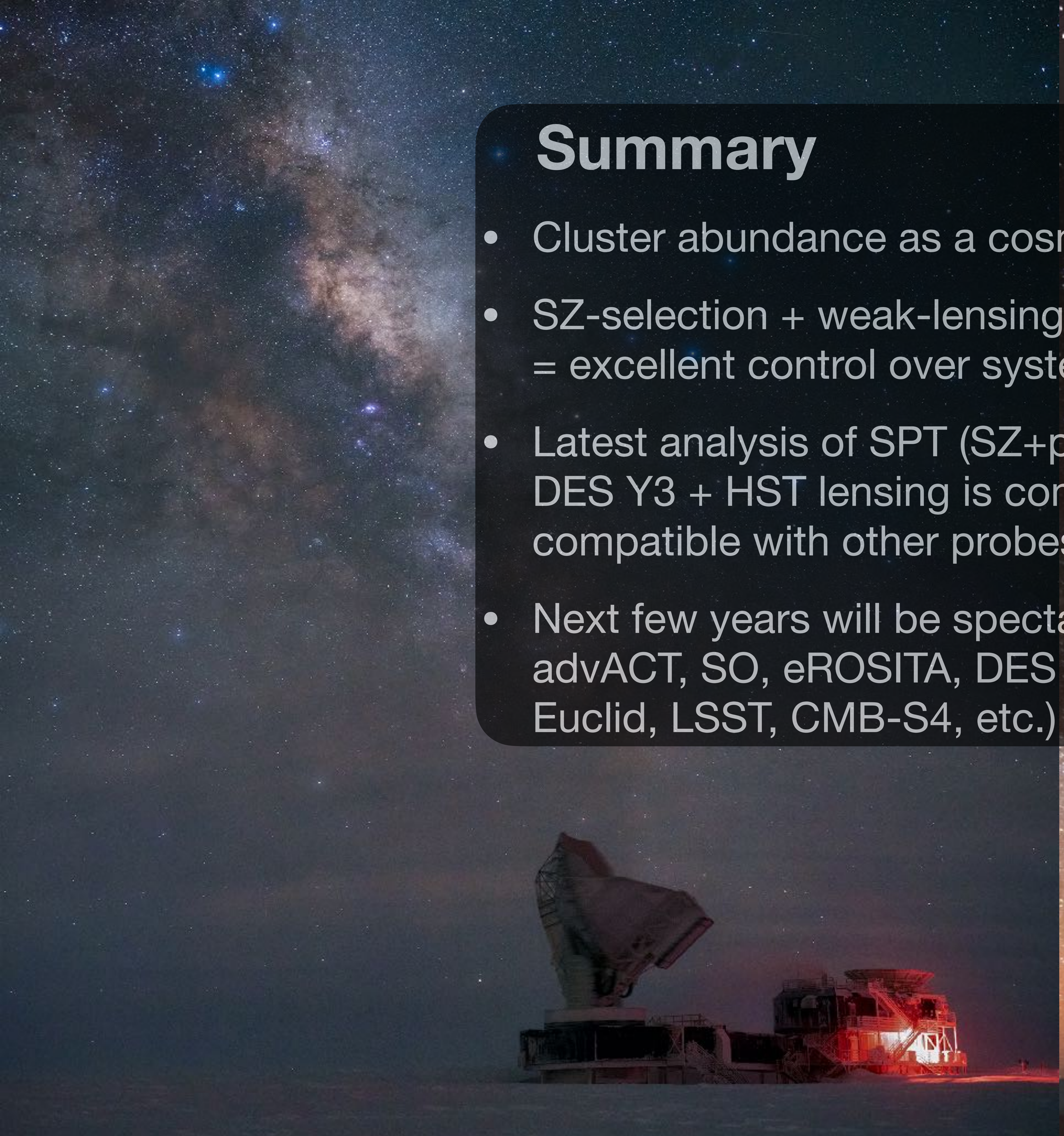

Image credit: Aman Chokshi

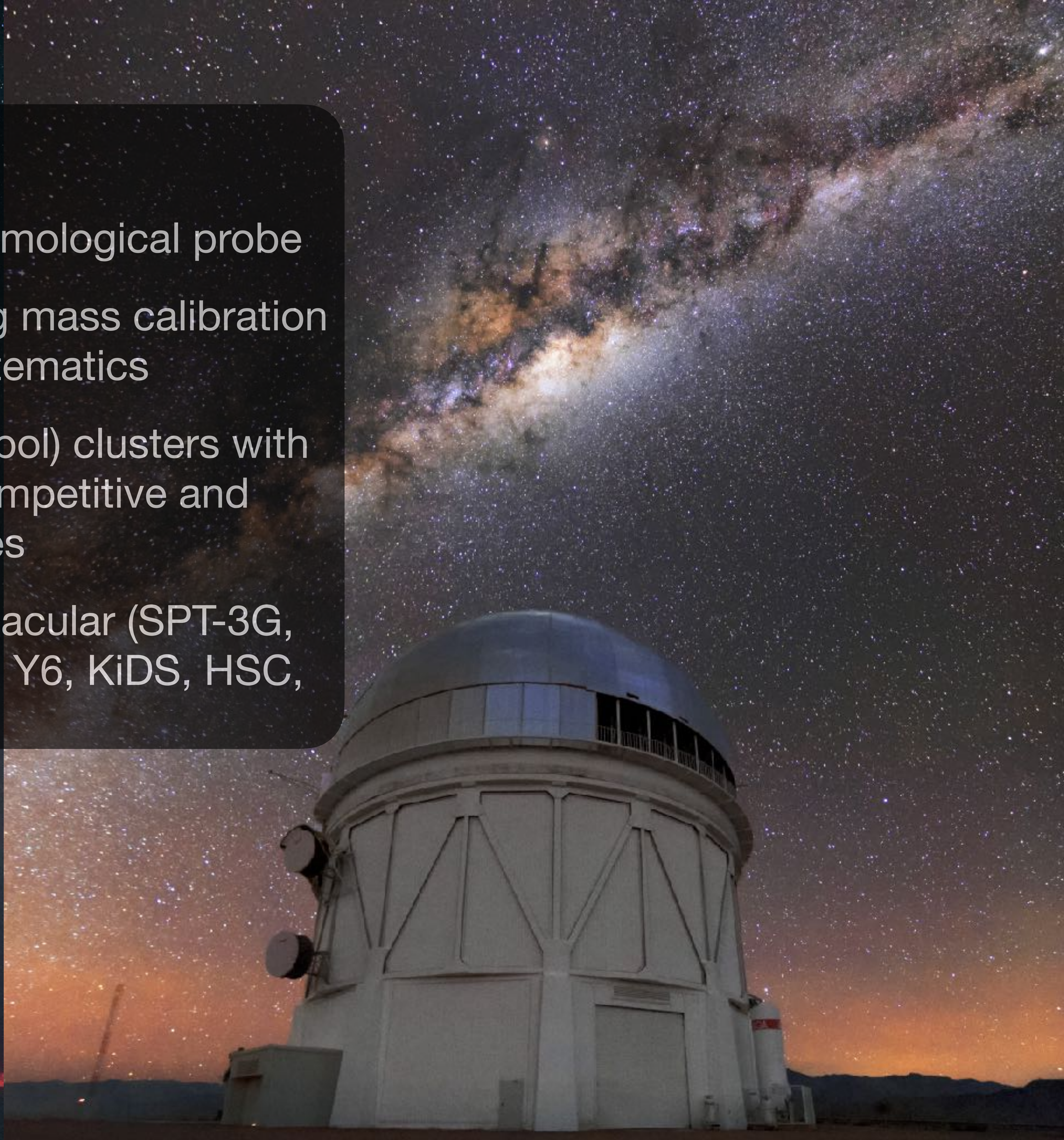

Image credit: CTIO/NOIRLab/NSF/AURA/D. Munizaga